Copy 6
RM E50F09

NACA

RESEARCH MEMORANDUM

ANALYTICAL DETERMINATION OF LOCAL SURFACE HEAT-TRANSFER COEFFICIENTS FOR COOLED TURBINE BLADES FROM MEASURED METAL TEMPERATURES

By W. Byron Brown and Jack B. Esgar

Lewis Flight Propulsion Laboratory
Cleveland, Ohio

NATIONAL ADVISORY COMMITTEE FOR AERONAUTICS

WASHINGTON
August 11, 1950

NACA RM E50F09

NATIONAL ADVISORY COMMITTEE FOR AERONAUTICS

RESEARCH MEMORANDUM

ANALYTICAL DETERMINATION OF LOCAL SURFACE HEAT-TRANSFER COEFFICIENTS FOR COOLED TURBINE BLADES FROM MEASURED METAL TEMPERATURES

By W. Byron Brown and Jack B. Esgar

SUMMARY

Analytical methods for the determination of local values of outside and inside heat-transfer coefficients and effective gas temperatures from turbine-blade-temperature measurements were developed. Temperature-distribution equations are derived for typical turbine-blade configurations at the central section when the wall thickness is uniform, at the leading-edge section, and at the trailing-edge section. The equations have the same general form for all sections of the blade, but the blade configuration at the location where the data measurements are taken affects the evaluation of some terms in the general equation.

Procedures for applying these analytical methods to experimentally measured blade-metal temperatures are presented. Data are presented for the leading and trailing edges of a symmetrical water-cooled blade to illustrate the validity of the methods for those portions of the blade.

In addition to the application to turbine blades, the methods can be applied to any heat-transfer apparatus having a profile that can be approximated by the shapes discussed.

INTRODUCTION

The development of a sound basis for the design of cooled turbines is dependent on knowledge of the inside and outside heat-transfer coefficients for turbine blades. Average heat-transfer coefficients can be determined for any particular blade configuration, but it appears infeasible at present to obtain a correlation of average coefficients that is suitable for all blade configurations at all temperature ratios and all velocity distributions. The fundamental

boundary-layer and heat-transfer theories are therefore being studied at the NACA Lewis laboratory as a means of predicting local heat-transfer coefficients for any given set of flow conditions. These studies will eliminate the necessity for experimental work on every conceivable blade shape.

In order to verify and to extend these theoretical studies, local heat-transfer coefficients around the periphery of a limited number of turbine blades must be determined over a wide range of flow conditions.

Three methods were proposed for obtaining these coefficients: (1) boundary-layer surveys using a hot-wire anemometer, (2) boundary-layer surveys using an optical interferometer, and (3) analytical solutions using measured turbine-blade temperatures. Considerable progress has been made in the development of operating techniques for the hot-wire anemometer and the interferometer, but some problems must still be solved. The third method is probably the best means presently available. A development of analytical solutions is presented herein for calculating local values of outside- and inside-convection heat-transfer coefficients from experimental data obtained at steady-state conditions from the measured temperatures of turbine blades having a known thermal conductivity.

METHODS OF ANALYZING HEAT-TRANSFER DATA TO OBTAIN LOCAL CONVECTION COEFFICIENTS AND EFFECTIVE GAS TEMPERATURES

The quantity of heat transferred per unit area by convection from a gas stream to a solid surface can be expressed as the product of the surface heat-transfer coefficient and the effective temperature difference between the gas and the surface. For one-dimensional heat flow, this same quantity of heat will be conducted through the wall of the solid and can be evaluated by multiplying the thermal conductivity of the wall material by the temperature gradient in the wall. If the inside of the wall is convection-cooled by a fluid, the heat transferred can also be expressed as the product of the inside-surface heat-transfer coefficient and the effective temperature difference between the inside surface and the coolant. By using this reasoning, a heat balance can be set up so that the inside and outside heat-transfer coefficients can be calculated from a known temperature difference between two known locations in the wall having a known thermal conductivity.

The temperature-distribution equations for any wall configuration where the heat flow is one dimensional can be reduced to the following form (Symbols are defined in appendix A and equations are derived in appendix B.):

$$t_x - t_y = \Gamma(t_e - t_x) \tag{1}$$

and

$$h_i = \frac{1}{\zeta\left(\frac{t_e - t_c}{t_e - t_B}\right) - \eta} \tag{2}$$

where

t_x and t_y wall temperatures at two specific locations lying in direction of heat flow

t_B wall temperature any place in line of heat flow (usually taken as either t_x or t_y)

Γ proportionality factor that is function of wall configuration, location of temperature measurements t_x and t_y, and ratio of outside heat-transfer coefficient h_t to wall thermal conductivity k_B; can be mathematically expressed and experimentally determined

ζ and η proportionality factors that are functions of wall configuration, location of temperature measurement t_B, wall thermal conductivity, and ratio of outside heat-transfer coefficient to wall thermal conductivity; can be mathematically expressed and evaluated by use of ratio h_t/k_B calculated from experimental determination of Γ

The mathematical expressions for Γ, ζ, and η are relatively simple for a simple shape such as a wall of uniform thickness, but they become more complicated for walls defined by concentric circles or for rectangular- or trapezoidal-shaped fins. Mathematical expressions for shapes other than those mentioned have not been derived. For a given configuration and thermocouple location, Γ, $k_B\zeta$, and $k_B\eta$ can be mathematically evaluated as functions of h_t/k_B and

plotted over the range of h_t/k_B that can be expected in experimental investigations. This fact greatly simplifies the use of these quantities.

From equation (1) it can be seen that if t_x, t_y, and t_e are known from experiment, the value of Γ is easily calculated. The quantity h_t/k_B can then be obtained for a mathematically determined curve of Γ as a function of h_t/k_B. For a known value of the thermal conductivity k_B, the outside heat-transfer coefficient h_t is then also known. The values of h_t/k_B and k_B can then be used to evaluate ζ and η, and if the coolant temperature t_c is known from experiment, the inside heat-transfer coefficient h_i can be calculated from equation (2).

Frequently the effective gas temperature t_e is unknown and will also have to be evaluated from experimental investigations. In order to evaluate t_e, a series of experimental data points must be obtained for a constant outside heat-transfer coefficient h_t. From equation (1), if $t_x - t_y$ is plotted against t_x for a constant value of Γ, the intercept on the t_x-axis will be t_e (this is the case where $t_x - t_y = 0$) and the slope of the plotted line will be $-\Gamma$. By using this method it is possible to determine both h_t (from $-\Gamma$) and t_e.

It is often more convenient to write equation (1) in the form

$$\frac{t_x - t_y}{t_g} = \Gamma\left(\Omega - \frac{t_x}{t_g}\right) \tag{3}$$

where t_g is an observed gas temperature, and

$$\Omega = \frac{t_e}{t_g} \tag{4}$$

From equation (3), if $(t_x - t_y)/t_g$ is plotted against t_x/t_g, the intercept on the t_x/t_g-axis will be Ω and the slope will again be $-\Gamma$. The effective gas temperature is then calculated from the value of Ω by use of equation (4), and the outside heat-transfer coefficient is determined from the slope $-\Gamma$.

Sometimes measuring the temperature at two points in the wall is impossible. If only one wall temperature t_B is known, the temperature-distribution equation for determining the outside heat-transfer coefficient can be written

$$t_B - t_c = \Gamma(t_e - t_c) \tag{5}$$

or

$$\frac{t_B - t_c}{t_g} = \Gamma\left(\Omega - \frac{t_c}{t_g}\right) \tag{6}$$

For the cases where the temperature gradient in the metal could be measured by means of two thermocouples, the term Γ was a function of h_t/k_B and the blade dimensions. For the case with one wall-temperature measurement, however, Γ is also a function of the inside heat-transfer coefficient h_i. Consequently, the method of applying equation (5) or (6) to experimental data is different from the method used for equations (1) and (3). The procedure is rather complex and has been utilized for a uniform wall thickness only; it is explained in detail in the section entitled "Application of Heat-Transfer Equations to Experimental Data."

The temperature-distribution equations used for all these analytical methods are based on a total outside-surface heat-transfer coefficient that is a combination radiation and convection coefficient. Corrections can be made to this total heat-transfer coefficient for radiant-heat transfer to obtain a true convection coefficient.

These methods of calculating heat-transfer coefficients and effective gas temperatures can be applied to any apparatus where the heat flow is one dimensional and the heat transfer is through a shape that can be approximated by the simple shapes discussed herein. The central section (with uniform wall thickness), the leading-edge section, and the trailing-edge section of most turbine blades can be approximated by simple shapes so that these methods of analysis can be used to determine local values of inside and outside heat-transfer coefficients and effective gas temperatures.

Central Section of Turbine Blade

Equations are presented for blades having a uniform wall thickness between the leading-edge and trailing-edge sections for plain hollow blades as shown in figures 1(a) and 1(b). Analyses for the central sections of other blade configurations have not been verified and therefore will not be presented here. The derivations for all equations are given in appendix B.

Case for measurable wall-temperature gradient. - In order to use this method, the wall temperature must be known at two points located in the line of heat flow.

The heat flow through the blade wall is assumed normal to the blade surface, and the surface curvature is assumed small enough that the wall can be treated as a flat plate. With the substitution of temperatures t_1 and t_2 at the locations shown by small circles on figure 1(a), equations (1) and (3) take the form

$$t_1 - t_2 = \Gamma(t_e - t_1) \tag{7}$$

and

$$\frac{t_1 - t_2}{t_g} = \Gamma\left(\Omega - \frac{t_1}{t_g}\right) \tag{8}$$

where

$$\Gamma = \frac{\frac{h_t}{k_B}(\delta_1 - \delta_2)}{1 + \frac{h_t}{k_B}(\bar{\delta} - \delta_1)} \tag{9}$$

The dimensions δ_1, δ_2, and $\bar{\delta}$ are shown in figure 1(a)

The values of ζ and η in equation (2) are

$$\zeta = \frac{1}{k_B}\left(\frac{k_B}{h_t} + \bar{\delta} - \delta_2\right) \tag{10}$$

and

$$\eta = \frac{1}{k_B}\left(\frac{k_B}{h_t} + \bar{\delta}\right) \tag{11}$$

Case with one temperature measurement in blade wall. - The temperature-distribution equation for the case with one thermocouple in a wall of uniform thickness can be written

$$t_B - t_c = \Gamma(t_e - t_c) \tag{5}$$

or

$$\frac{t_B - t_c}{t_g} = \Gamma\left(\Omega - \frac{t_c}{t_g}\right) \tag{6}$$

where

$$\Gamma = \frac{h_t(k_B + \delta\, h_i)}{k_B(h_t + h_i) + \bar{\delta}\, h_t h_i} \tag{12}$$

The dimensions δ and $\bar{\delta}$ are shown in figure 1(b).

As previously mentioned, Γ is a function of h_t/k_B and h_i as well as of blade configuration and thermocouple location. In order to maintain Γ constant, the term h_i in equation (12) should be replaced by a quantity that can be maintained at a constant value. In general, the inside heat-transfer coefficient is proportional to the coolant flow raised to some power if the coolant temperature is constant, that is

$$h_i = C w_c^n \tag{13}$$

Equation (12) now becomes

$$\Gamma = \frac{h_t(k_B + \delta C w_c^n)}{k_B(h_t + C w_c^n) + \bar{\delta} h_t C w_c^n} \tag{14}$$

Equation (14) can also be written

$$\frac{1-\Gamma}{w_c^n} = \Gamma\left(\frac{C}{h_t} + \frac{\bar{\delta}C}{k_B}\right) - \frac{\delta C}{k_B} \tag{15}$$

The application of equations (5), (6), and (15) to experimental heat-transfer data will be discussed later.

The value of the inside heat-transfer coefficient can be obtained from equation (2) where

$$\zeta = \frac{1}{k_B}\left(\frac{k_B}{h_t} + \bar{\delta} - \delta\right) \tag{16}$$

$$\eta = \frac{1}{k_B}\left(\frac{k_B}{h_t} + \bar{\delta}\right) \tag{17}$$

Leading-Edge Section of Turbine Blade

The heat is assumed to be transmitted from the gas stream through the blade at the leading edge to the coolant along a sector having an included angle $d\theta$, as shown in the cross-sectional view of the leading-edge section in figure 1(c), where thermocouples 3 and 4, indicated by small circles, lie in a direct line between the stagnation point on the blade surface and the coolant passage. The equation for the temperature distribution at the leading edge can be written

$$t_3 - t_4 = \Gamma(t_e - t_3) \tag{18}$$

or

$$\frac{t_3 - t_4}{t_g} = \Gamma\left(\Omega - \frac{t_3}{t_g}\right) \tag{19}$$

and

$$\Gamma = \frac{\frac{r_o h_t}{k_B} \log_e \frac{r_3}{r_4}}{1 + \frac{r_o h_t}{k_B} \log_e \frac{r_o}{r_3}} \tag{20}$$

where

r radii as shown with subscripts on figure 1(c)

The values of ζ and η in equation (2) are

$$\zeta = \frac{r_i}{k_B}\left(\frac{k_B}{h_t r_o} + \log_e \frac{r_o}{r}\right) \tag{21}$$

and

$$\eta = \frac{r_i}{k_B}\left(\frac{k_B}{h_t r_o} + \log_e \frac{r_o}{r_i}\right) \tag{22}$$

Trailing-Edge Section of Turbine Blade

A cross section of the trailing-edge section of most turbine blades can be very closely approximated by a trapezoid, a rectangle, or a combination of trapezoids and rectangles. Temperature distributions have been determined for rectangular and trapezoidal cross sections where the heat flow is assumed to be one dimensional. Derivations are given in appendix B for trailing-edge sections composed of the following shapes:

1. Trapezoidal

2. Rectangular

3. Combination of one trapezoid and one rectangle

4. Combination of two trapezoids

Equations for Γ, ξ, and η are given for each of the shapes.

Trapezoidal trailing-edge section. - By referring to the trapezoidal trailing-edge section on figure 1(d) for thermocouple locations and dimensions, equations (1) and (3) can be written

$$t_5 - t_6 = \Gamma(t_e - t_5) \tag{23}$$

and

$$\frac{t_5 - t_6}{t_g} = \Gamma\left(\Omega - \frac{t_5}{t_g}\right) \tag{24}$$

where

$$\Gamma = \frac{N_6 - N_5}{N_5} \tag{25}$$

The values of ξ and η in equation (2) are

$$\xi = \frac{N}{I} \tag{26}$$

and

$$\eta = \frac{E}{I} \tag{27}$$

where

$$N = \frac{\xi_2}{2B^2 k_B}\left[H_1(i\xi_1)\, J_0(i\xi) + iJ_1(i\xi_1)\, iH_0(i\xi)\right] \tag{28}$$

$$I = iJ_1(i\xi_1)\, H_1(i\xi_2) - H_1(i\xi_1)\, iJ_1(i\xi_2) \tag{29}$$

$$E = \frac{\xi_2}{2B^2 k_B}\left[H_1(i\xi_1)\, J_0(i\xi_2) + iJ_1(i\xi_1)\, iH_0(i\xi_2)\right] \tag{30}$$

$$\xi = 2B\sqrt{\left(y + \frac{\pi}{4}\tau_1\right) + \tau_1\left(\frac{1 - \tan\alpha}{2\tan\alpha}\right)}$$

$$B^2 = \frac{h_t}{k_B \sin\alpha}$$

and

$$\alpha = \tan^{-1}\frac{\tau_3 - \tau_1}{2L}$$

N_5 evaluated for $y = y_5$

N_6 evaluated for $y = y_6$

ξ_1 evaluated for $y + \frac{\pi\tau_1}{4} = 0$

ξ_2 evaluated for $y = L$

y, τ_1, τ_3, L shown on trailing-edge section sketch for trapezoidal shape (fig. 1(d))

Where there are no subscripts on N and ξ, they can be evaluated for either thermocouple in the trailing-edge section. The resulting value of h_i in equation (2) should be the same in either case.

Rectangular trailing-edge section. - For the rectangular trailing-edge section as illustrated by the trailing-edge section shown in combination with a trapezoidal section in figure 1(e), equations (1) and (3) are written

$$t_5 - t_7 = \Gamma(t_e - t_5) \tag{31}$$

and

$$\frac{t_5 - t_7}{t_g} = \Gamma\left(\Omega - \frac{t_5}{t_g}\right) \tag{32}$$

and

$$\Gamma = \frac{\cosh\varphi\left(y_7 + \frac{\pi}{4}\tau_1\right) - \cosh\varphi\left(y_5 + \frac{\pi}{4}\tau_1\right)}{\cosh\varphi\left(y_5 + \frac{\pi}{4}\tau_1\right)} \tag{33}$$

The values of ζ and η in equation (2) are

$$\zeta = \frac{\cosh \varphi\left(y + \frac{\pi}{4}\tau_1\right)}{k_B\varphi \sinh \varphi\left(L_2 + \frac{\pi}{4}\tau_1\right)} \tag{34}$$

and

$$\eta = \frac{\cosh \varphi\left(L_2 + \frac{\pi}{4}\tau_1\right)}{k_B\varphi \sinh \varphi\left(L_2 + \frac{\pi}{4}\tau_1\right)} \tag{35}$$

where

$$\varphi = \sqrt{\frac{2h_t}{k_B\tau_1}}$$

The dimensions y, τ, and L are shown in figure 1(e).

Combination trapezoidal and rectangular trailing-edge section. - For rectangular portion d of the trailing-edge section shown on figure 1(e), the value of Γ is the same as in equation (33).

$$\Gamma = \Gamma_d = \frac{\cosh \varphi_d\left(y_7 + \frac{\pi}{4}\tau_1\right) - \cosh \varphi_d\left(y_5 + \frac{\pi}{4}\tau_1\right)}{\cosh \varphi_d\left(y_5 + \frac{\pi}{4}\tau_1\right)} \tag{33a}$$

For the trapezoidal portion b,

$$t_7 - t_6 = \Gamma_b(t_e - t_7) \tag{36}$$

or

$$\frac{t_7 - t_6}{t_g} = \Gamma_b\left(\Omega - \frac{t_7}{t_g}\right) \tag{37}$$

and

$$\Gamma_b = \frac{J_0(i\xi_{b,6}) - J_0(i\xi_{b,7}) + \frac{dZ}{dK}\left[iH_0(i\xi_{b,6}) - iH_0(i\xi_{b,7})\right]}{J_0(i\xi_{b,7}) + \frac{dZ}{dK}\, iH_0(i\xi_{b,7})} \tag{38}$$

where

$$\frac{dZ}{dK} = \frac{2B_b^2 iJ_1\left(i\xi_{b,1}\right) + \xi_{b,1}\,\varphi_d\left[\tanh\varphi_d\left(L_2 + \frac{\pi}{4}\tau_1\right)\right]J_0\left(i\xi_{b,1}\right)}{2B_b^2 H_1\left(i\xi_{b,1}\right) - \xi_{b,1}\,\varphi_d\left[\tanh\varphi_d\left(L_2 + \frac{\pi}{4}\tau_1\right)\right]iH_0\left(i\xi_{b,1}\right)} \tag{39}$$

$$\xi_b = 2B_b\sqrt{y + \tau_1\left(\frac{1-\tan\alpha_b}{2\tan\alpha_b}\right)}$$

$$\alpha_b = \tan^{-1}\frac{\tau_3 - \tau_1}{2L_1}$$

and $\xi_{b,1}$ is evaluated for $y = 0$. The subscript b refers to portion b of trailing-edge section.

The value of Γ_b in equation (38) is a function of both $h_{t,b}/k_B$ and $h_{t,d}/k_B$. For the most accurate solution to the equation, it is necessary to evaluate dZ/dK in equation (39) using the value of $h_{t,d}/k_B$ obtained for the rectangular portion of the trailing edge by use of equation (33a). It is doubtful that this much trouble is warranted, however, because the terms in equation (38) involving dZ/dK are small compared with the other terms in the equation so that the error caused by assuming $h_{t,d} = h_{t,b}$ would be negligible. By using this assumption, Γ_b can be evaluated as a function of $h_{t,b}$ only.

The method for determining the value of h_i at the trailing-edge where the section is composed of two different portions is so insensitive to the metal-temperature measurements that the analytical solution is not believed to be worthwhile and therefore is not presented. The determination of h_i is much more accurate at the central portion of the blade where the shape factor is simpler. The evaluation of the outside coefficient h_t is considered to be quite accurate at the trailing-edge section, however. Because such a small portion of the coolant passage is next to the trailing-edge section, the evaluation of the inside heat-transfer coefficient at that portion of the blade is of minor importance.

Combination of two trapezoidal portions in trailing-edge section. - For trapezoidal portion d' on figure 1(f),

$$t_5 - t_7 = \Gamma_{d'}(t_e - t_5) \tag{40}$$

or

$$\frac{t_5 - t_7}{t_g} = \Gamma_{d'}\left(\Omega - \frac{t_5}{t_g}\right) \tag{41}$$

and

$$\Gamma_{d'} = \frac{N_7 - N_5}{N_5} \tag{42}$$

where

$$N = \frac{\xi_{d',2}}{2B_{d'}{}^2 k_B}\left[H_1(i\xi_{d',1})\, J_0(i\xi_{d'}) + iJ_1(i\xi_{d',1})\, iH_0(i\xi_{d'})\right]$$

$$B_{d'}{}^2 = \frac{h_t}{k_B \sin \alpha_{d'}}$$

$$\xi_{d'} = 2B_{d'}\sqrt{\left(y + \frac{\pi}{4}\tau_1\right) + \tau_1\left(\frac{1 - \tan \alpha_{d'}}{2 \tan \alpha_{d'}}\right)}$$

and

$$\alpha_{d'} = \tan^{-1}\frac{\tau_2 - \tau_1}{2L_2}$$

For trapezoidal portion b' on figure 1(f),

$$t_7 - t_6 = \Gamma_{b'}(t_e - t_7) \tag{43}$$

or

$$\frac{t_7 - t_6}{t_g} = \Gamma_{b'}\left(\Omega - \frac{t_7}{t_g}\right) \tag{44}$$

and

$$\Gamma_{b'} = \frac{J_0(i\xi_{b',6}) - J_0(i\xi_{b',7}) + \frac{dZ'}{dK'}\left[iH_0(i\xi_{b',6}) - iH_0(i\xi_{b',7})\right]}{J_0(i\xi_{b',7}) + \frac{dZ'}{dK'} iH_0(i\xi_{b',7})} \tag{45}$$

where

$$\frac{dZ'}{dK'} = \frac{GiJ_1(i\xi_{b',1}) + SJ_0(i\xi_{b',1})}{GH_1(i\xi_{b',1}) - SiH_0(i\xi_{b',1})} \tag{46}$$

$$G = J_0(i\xi_{d',2}) + \frac{iJ_1(i\xi_{d',1})iH_0(i\xi_{d',2})}{H_1(i\xi_{d',1})}$$

and

$$S = \frac{B_{d'}{}^2\xi_{b',1}}{B_{b'}{}^2\xi_{d',1}}\left[\frac{iJ_1(i\xi_{d',1})\, H_1(i\xi_{d',2})}{H_1(i\xi_{d',1})} - iJ_1(i\xi_{d',2})\right]$$

Also

$$\xi_{b'} = 2B_{b'}\sqrt{y + \tau_2\left(\frac{1 - \tan\alpha_{b'}}{2\tan\alpha_{b'}}\right)}$$

and

$$\alpha_{b'} = \tan^{-1}\frac{\tau_3 - \tau_2}{2L_1}$$

where

$\xi_{b',6}$ evaluated for $y = y_6$

$\xi_{b',7}$ evaluated for $y = y_7$ ($y_7 = 0$ for this case)

$\xi_{b',1}$ evaluated for $y = 0$

$\xi_{d',2}$ evaluated for $y = L_2$

$\xi_{d',1}$ evaluated for $y + \frac{\pi r_1}{4} = 0$

A method of evaluating h_i for this section of the blade is not presented for reasons previously discussed.

Radiation Corrections

The effects of radiation have been neglected up to this point in the analysis so that the local outside heat-transfer coefficients obtained are combination convection and radiation coefficients. In most cases, the heat transferred by radiation is relatively small (about 3 to 10 percent of the heat transferred by convection for uncooled surface temperatures up to 1500° F), but it is still of sufficient magnitude to require evaluation.

The combination convection and radiation coefficient has been defined as h_t; if the convection coefficient is designated h_o and the radiation coefficient, h_r, the following equations may be written:

$$h_t = h_o + h_r \tag{47}$$

and

$$h_t = \frac{Q_t}{A_{B,o}(t_e - t_B)} = \frac{Q + Q_r}{A_{B,o}(t_e - t_B)} \tag{48}$$

where

Q_t total heat-flow rate to blade

Q heat-flow rate to blade by convection

Q_r heat-flow rate to blade by radiation

The heat transferred by radiation is given in reference 1 as

$$Q_r = 0.173\, A_{B,o}\, \mathcal{F} \left[\left(\frac{t_w}{100} \right)^4 - \left(\frac{t_B}{100} \right)^4 \right] \tag{49}$$

therefore

$$h_r = \frac{0.173\mathscr{F}\left[\left(\frac{t_w}{100}\right)^4 - \left(\frac{t_B}{100}\right)^4\right]}{t_e - t_B} \tag{50}$$

where

$$\mathscr{F} = \frac{1}{\frac{1}{F} + \left(\frac{1}{\epsilon_w} - 1\right) + \frac{A_w}{A_{B,o}}\left(\frac{1}{\epsilon_B} - 1\right)} \tag{51}$$

The actual value of the convection heat-transfer coefficient h_o can now be calculated for each gas temperature from equations (47) and (50).

A comprehensive discussion of radiation is unwarranted here. For a precise evaluation of radiation, it is necessary to accurately determine the geometry factor F and the emmissivities. A method of determining geometry factors by the use of a mechanical integrator on large-scale models is suggested by Hottel in reference 2. For most applications with cooled turbine blades, the metal surfaces will be tarnished and soot covered so that the emmissivity will be high, probably ranging from 0.80 to 0.95 for nearly all materials.

APPLICATION OF HEAT-TRANSFER EQUATIONS TO EXPERIMENTAL DATA

There are two methods of applying the heat-transfer equations to experimental heat-transfer data. The first method, which is the more direct and probably the better method, depends upon a knowledge of the effective gas temperature. The usual method of determining the effective gas temperature is calculation by use of a known blade recovery factor. A discussion of recovery factors is contained in reference 3. When the effective gas temperature, the measured blade temperature at two positions in the direction of heat flow, and the metal thermal conductivity are known, the outside and inside heat-transfer coefficients can be calculated directly. The second method can be used if the effective gas temperature is unknown, but data are necessary from heat-transfer runs where the heat-transfer coefficient on the outside surface of the blade is maintained constant while the amount of heat transfer to the blade is varied by allowing the coolant flow and either the coolant temperature or the gas temperature to change.

The second method cannot be used to determine the effective gas temperature with as great an accuracy as is possible using a local blade recovery factor. The method is therefore best applied when other means of determining effective gas temperature fail, such as the case where temperature gradients in the gas stream make measuring the stream temperature at the blade impossible.

Case with Known Effective Gas Temperature and Measurable Wall-Temperature Gradient

The effective gas temperature, or the gas temperature effecting heat transfer, is defined as the adiabatic surface temperature in reference 3; that is, the effective gas temperature is the temperature that the surface would assume if it were thermally insulated so that there would be no heat transfer. The local effective gas temperature can be calculated from the total gas temperature, the total pressure, and the local static pressure if the local blade recovery factor is known. For simple shapes such as flat plates, tubes, and wedges, analytical solutions for the recovery factor are available (reference 3). For more complex shapes, such as turbine blades, recovery factors can be determined from adiabatic tests of the blades. Experimental work at the Lewis laboratory has shown that turbine-blade recovery factors are usually quite close to 0.90 for all Reynolds numbers and for local Mach numbers from 0.4 to 1.0. The effective gas temperature is then

$$t_e = t + \Lambda_B(T - t) \tag{52}$$

or

$$t_e = T\left\{1 - (1 - \Lambda_B)\left[1 - \left(\frac{p}{P}\right)^{\frac{\gamma-1}{\gamma}}\right]\right\} \tag{52a}$$

In actual practice for subsonic flow, the value of the effective gas temperature t_e will be

$$0.98\ T < t_e \leq T$$

so that in many cases the error in assuming $t_e = T$ will be negligible. The size of the error will be dependent on the temperature difference $t_e - t_x$. A more complete discussion of this error will be found in the section entitled "Accuracy Considerations."

Equation (1) can be written

$$\Gamma = \frac{t_x - t_y}{t_e - t_x} \tag{1a}$$

so that Γ can be evaluated directly from the effective gas temperature and the measured blade temperatures. For a given configuration and given thermocouple locations, Γ can be mathematically represented as a function of h_t/k_B so that the heat-transfer coefficient h_t can be easily calculated. The inside heat-transfer coefficient h_i can then be evaluated from

$$h_i = \frac{1}{\zeta\left(\frac{t_e - t_c}{t_e - t_B}\right) - \eta} \tag{2}$$

where ζ and η are obtained from mathematically determined curves of $k_B\zeta$ and $k_B\eta$ plotted against h_t/k_B for the given configuration and thermocouple location.

Case with Unknown Effective Gas Temperature and Measurable Wall-Temperature Gradient

The method of application for this case is considerably more complex than for the case where the effective gas temperature is known. As previously stated, a constant heat-transfer coefficient must be maintained on the outside surface of the blade for a series of experimental heat-transfer runs in order to utilize this method of analysis. If the coolant flow and the coolant temperature are allowed to vary for a series of runs, the outside heat-transfer coefficient can be held constant by maintaining the gas flow and the gas temperature constant. The values of inside and outside heat-transfer coefficients and the effective gas temperature can then be obtained rather easily by use of equation (1)

$$t_x - t_y = \Gamma(t_e - t_x) \tag{1}$$

which can be solved by use of suitable plots. If $t_x - t_y$ (ordinate) is plotted against t_x at a constant value of Γ (constant h_t/k_B) over a range of blade-metal temperatures, the slope of the resulting line will be $-\Gamma$ and the intercept on the t_x-axis will be the

effective gas temperature t_e. The value of the local outside heat-transfer coefficient h_t can now be calculated from the equation for Γ for the section of the blade in question.

In order to obtain a sufficient number and a suitable range of temperatures t_x and t_y to determine the line in the plot of $t_x - t_y$ against t_x, it is necessary to vary both the coolant flow and the coolant temperature over as wide a range as possible.

After determining h_t and t_e, the value of the local inside heat-transfer coefficient h_i can be determined from equation (2). The values of ζ and η are evaluated as functions of h_t/k_B for the section of the blade.

If no provision is made for varying the coolant temperature, the gas temperature must be varied. The outside-surface heat-transfer coefficient is apparently affected by the ratio of gas temperature to blade temperature; therefore it may be necessary that the weight rate of gas flow be varied at the same time the gas temperature is varied in order to maintain a constant value of outside-surface heat-transfer coefficient. By making heat-transfer runs over a large range of gas flow and gas temperature, the effect of the ratio of gas to blade temperature can be determined so that data for a constant value of the outside-surface heat-transfer coefficient can be obtained for the required plots.

This effect can be evaluated if the variation in average convection coefficients with temperature ratio is assumed to be the same as the variation in local convection coefficients. This assumption will be valid if the point of transition from laminar to turbulent boundary-layer flow on the outside surface of the blade remains at the same place for all temperature ratios. Evidence exists indicating that the amount of laminarity is a function of temperature ratio unless the pressure gradient is strong enough to maintain a completely laminar boundary layer. Where the pressure gradient would indicate that the boundary layer is either almost completely laminar or almost completely turbulent, the following procedure can be used for evaluating the effect of temperature ratio on the outside heat-transfer coefficient:

1. The average outside heat-transfer coefficient $h_{t,av}$ can be calculated from the equation

$$h_{t,av} = \frac{c_{p,c} w_c \Delta t_c}{A_o (t_e - t_{B,av})}$$

where

$t_e = 0.98\ t_g$ (assumed value of $\Omega = 0.98$ as an approximation)

Then $h_{t,av}$ can be plotted against the weight rate of gas flow w_g for various measured gas temperatures t_g as shown in figure 2(a), Plot I.

2. From Plot I, a cross plot can be made as shown in figure 2(b), Plot II, to obtain t_g as a function of w_g for various values of $h_{t,av}$.

3. Local blade temperature t_B and coolant temperature t_c can be plotted against w_g for the various measured gas temperatures at a constant coolant flow, as shown in figures 2(c) and 2(d), Plots III and IV, respectively.

From Plots II, III, and IV, it is possible to correlate the weight rate of gas flow and the temperatures of the blade, coolant, and gas for given constant values of $h_{t,av}$ and coolant flow. These plots are required for obtaining temperatures to use in additional plots to determine outside and inside heat-transfer coefficients and effective gas temperatures.

By use of equation (3)

$$\frac{t_x - t_y}{t_g} = \Gamma\left(\Omega - \frac{t_x}{t_g}\right) \tag{3}$$

it can be seen that if $(t_x - t_y)/t_g$ (ordinate) is plotted against t_x/t_g for a wide range of gas temperatures and coolant flows at a constant value of $h_{t,av}$, the slope of the resulting line will be $-\Gamma$ and the intercept on the t_x/t_g—axis will be Ω. The values of t_y, t_x, and t_g are obtained from graphs like Plots II and III of figure 2.

The value of the local outside heat-transfer coefficient h_t can be obtained as before from the equation for Γ for the section of the blade in question, and the effective gas temperature is calculated from

$$t_e = \Omega t_g \tag{4a}$$

In order to simplify the evaluation of h_t from a known value of Γ, it is convenient to plot Γ as a function of h_t/k_B for the particular section of the blade, as previously explained.

The value of the local inside heat-transfer coefficient h_i can be determined from equation (2) where the value of t_c is obtained from Plot IV of figure 2, h_t and t_e are determined from equation (3), and the values of ζ and η are evaluated as functions of h_t/k_B for the blade section.

Case with Known Effective Gas Temperature and One Temperature Measurement in Blade Wall

Equation (5) can be written

$$\Gamma = \frac{t_B - t_c}{t_e - t_c} \tag{5a}$$

so that Γ can be evaluated directly from the effective gas temperature, the coolant temperature, and the blade temperature. Because Γ is a function of both h_i and h_t/k_B, a plot is necessary to determine the outside heat-transfer coefficient h_t. The data for this plot must be obtained from a series of experiments where the outside heat-transfer coefficient is maintained constant while the coolant flow is varied, which varies the inside heat-transfer coefficient. The value of Γ is then calculated from equation (5a) for each experimental point. The mathematical expression for Γ is

$$\Gamma = \frac{h_t(k_B + \delta\, h_i)}{k_B(h_t + h_i) + \overline{\delta}\, h_t h_i} \tag{12}$$

which can be written

$$\frac{1 - \Gamma}{w_c{}^n} = \Gamma\left(\frac{C}{h_t} + \frac{\overline{\delta C}}{k_B}\right) - \frac{\delta C}{k_B} \tag{15}$$

where h_i was replaced by $Cw_c{}^n$. The exponent n can be evaluated from calculations of the product of the average inside coefficient and the coolant-passage area for the variable coolant-flow runs. (The area need not be evaluated as it is constant.)

$$A_i h_{i,av} = \frac{c_{p,c}\, w_c \Delta t_c}{t_{B,av} - t_c} \qquad (53)$$

If $A_i h_{i,av}$ is plotted against w_c on logarithmic coordinates, the slope of the resulting line is the exponent n.

It can be seen from equation (15) that if $(1 - \Gamma)/w_c^n$ is plotted against Γ for variable coolant-flow runs, the intercept on the Γ-axis of the resulting straight line is Γ' (for $(1 - \Gamma)/w_c^n = 0$). Substitution of this value of Γ' into equation (15) yields

$$\frac{h_t}{k_B} = \frac{\Gamma'}{\delta - \bar{\delta}\Gamma'} \qquad (54)$$

from which the value of h_t can be calculated.

The local inside heat-transfer coefficient h_i is then calculated from equation (2) using equations (16) and (17) to evaluate ζ and η, respectively.

This method of determining heat-transfer coefficients using only one blade-metal-temperature measurement, however, is not completely satisfactory in all cases. The method works best for blades made of metals having low thermal conductivities. When the blade metal is thin and the metal thermal conductivity is high, obtaining an accurate evaluation of the outside coefficient h_t becomes difficult, although the ratio of inside to outside coefficients can be quite accurately evaluated. If the local inside coefficient h_i can be obtained from measurements in the coolant passage, the value of h_t can then quite easily be obtained from equations (5a) and (12).

Case with Unknown Effective Gas Temperature and One Temperature Measurement in Blade Wall

When the effective gas temperature is unknown, the experimental values of local heat-transfer coefficient and effective gas temperature are obtained from a graphical solution of equation (6)

$$\frac{t_B - t_c}{t_g} = \Gamma\left(\Omega - \frac{t_c}{t_g}\right) \qquad (6)$$

as illustrated in figure 3. In Plot I (fig. 3(a)), $(t_B - t_c)/t_g$ is plotted against t_c/t_g for various constant values of coolant flow (and thus constant h_i), where t_c, t_g, and t_B are obtained from plots like those in figure 2 for a constant value of $h_{t,av}$.

The slope of each line is $-\Gamma$ and the intercept of all lines on the t_c/t_g-axis is Ω. The effective gas temperature t_e can now be calculated from

$$t_e = \Omega t_g \tag{4a}$$

The graphical solution to equation (15) is illustrated in Plot II (fig. 3(b)). The values of Γ for corresponding values of w_c are obtained from Plot I (fig. 3(a)). The straight line representing the plotted values of Γ against $(1 - \Gamma)/w_c^n$ on Plot II can be extended to intercept the Γ-axis at a point denoted by Γ', as previously explained. The value of h_t can then be calculated from equation (54). The local inside heat-transfer coefficient h_i is then calculated from equation (2) in the same manner as previously explained. Again, this method is not completely satisfactory for all cases, particularly when the metal thermal conductivity is high.

ACCURACY CONSIDERATIONS

In the experimental determination of heat-transfer coefficients from cooled turbine blades, sources of error exist in the experimental measurements and in the method of analysis that must be minimized. These possible sources of error are:

1. Assumption of one-dimensional heat transfer

2. Effect of approximations to blade configuration

3. Effect of variations of thermal conductivity in direction of heat flow

4. Effect of variation in heat-transfer coefficient along blade in chordwise direction

5. Effect of temperature gradient in trailing-edge section

6. Accuracy required in locating thermocouples

7. Effect of thermocouple hole on heat-flow path

8. Accuracy of temperature measurement

Each of the preceding items is discussed in detail.

Assumption of One-Dimensional Heat Transfer

Errors in the assumption of one-dimensional flow are negligible except near the rim on a cooled turbine, as shown in references 4 and 5. The lower the metal thermal conductivity, the smaller the errors involved. The metals used in nearly all turbines do have a low conductivity. In static-cascade work, some means of thermally insulating the ends of the blades is usually used so that spanwise temperature gradients are minimized even at the blade ends.

The temperature distribution through the cross section of a typical water-cooled turbine blade was computed by relaxation methods (reference 6) for two metal thermal conductivities and for both a constant and a variable outside heat-transfer coefficient. In all cases, the isothermal lines showed that the heat flow was very close to being one dimensional at the leading and trailing edges. It was also found that the temperature distribution in the trailing-edge section of the blade could be accurately determined by a calculation of the temperature distribution through a wedge of comparable dimensions.

At the central section (midchord) of a blade with a uniform wall thickness, the heat flow will be one dimensional except at the ends of the coolant passage next to the leading- and trailing-edge sections. At such locations, where the flow is known to be two or three dimensional, these analytical methods should not be used.

The assumption of one-dimensional heat flow is valid when reasonable care is used in locating thermocouples in regions away from end effects.

Effect of Approximations to Blade Configuration

As previously mentioned, the temperature distribution in the trailing-edge section can be accurately determined by a calculation of the temperature distribution through a wedge (trapezoidal trailing-edge section) of comparable dimensions (reference 6). Conversely, if

the temperature distribution is known (defined herein by two temperatures at two known locations), the outside heat-transfer coefficient can be accurately determined. The same assumption of one-dimensional heat flow is used for a rectangular trailing edge, and therefore the same accuracy should be obtained. Trailing-edge cross sections can usually be approximated very closely by some combination of rectangles and trapezoids, so that errors due to shape approximations can be made negligible.

At the leading edge of the blade, the accuracy will depend upon the configuration. If the leading edge is well rounded, relaxation calculations indicate that the shape approximation of two concentric arcs will give results accurate to about 10 percent. The application of the leading-edge analysis is less accurate than the application of analyses for the central and trailing-edge sections because the shape approximation is not completely valid.

The assumption that the central portion of the blade can be approximated by a flat plate is accurate for large radii of curvature. For small radii of curvature at the central portion of the blade, more accurate results can be obtained by use of the leading-edge equations for arcs of concentric circles. The leading-edge equation approaches the central-section equation as the radius approaches infinity. The approximate percentage error involved in using the flat-plate equation for determining Γ can be determined from the expression

$$\text{Error(percent)} \approx 100 \frac{\overline{\delta}}{2r_o} \tag{55}$$

where

$\overline{\delta}$ wall thickness

r_o radius of curvature of outside surface of blade

For a given value of Γ, the calculated heat-transfer coefficient h_t is always higher for the flat-plate equation.

Effect of Variations of Thermal Conductivity in Direction of Heat Flow

The analytical methods were derived with the assumption that the section of the blade in question was of a material having a uniform thermal conductivity. The thermal conductivity of a material

is a function of its temperature. There must be a temperature gradient to have heat flow; therefore the thermal conductivity varies in the direction of heat flow. Analyses have been made to evaluate the effect of variable thermal conductivity caused by temperature gradients. For a typical high-temperature-metal alloy with the thermal conductivity given by

$$k = 2.763 \times 10^{-6}T + 1.246 \times 10^{-3} \qquad (56)$$

the temperature distribution was calculated for temperature differences as high as 130° F between two points in the metal. The error caused by using an average metal temperature for evaluating the thermal conductivity was negligible.

If the blade is laminated or coated on the inside or outside so that a nonuniform thermal conductivity is caused by the use of different materials, a great deal of care will be required in interpreting the results of the analysis. The heat flow can still be measured as long as the temperature measurements are made in a piece of material of constant thermal conductivity, but the heat-transfer coefficients obtained from the analysis will contain the effects of convection, radiation, and conduction through the material having a thermal conductivity different from the material in which the temperature measurements are made.

Effect of Variation in Heat-Transfer Coefficient along Blade in Chordwise Direction

At the leading edge of the blade where the heat-transfer coefficient changes rapidly with the distance from the stagnation point, the determination of the outside heat-transfer coefficient will be inaccurate unless the thermocouples used to measure the temperature gradient lie in a direct line between the stagnation point and the coolant passage. If the leading-edge section is long and relatively sharp, the results obtained from the analysis will be of very doubtful quality. The analysis method is based on a short, well-rounded leading-edge section.

At the central and trailing-edge sections of the blade, the variation in heat-transfer coefficient in a chordwise direction is usually gradual so that its effect will be quite small. At the central portion of the blade the effect will be negligible and at the trailing-edge section the calculated heat-transfer coefficient will be an average value for the blade surface between two thermocouple stations. The closer these stations are together, the smaller will be the effect of variation in heat-transfer coefficient.

Effect of Temperature Gradient in Trailing-Edge Section

A decrease occurs in the magnitude of local heat-transfer coefficients as the surface temperature of a flat plate increases in the direction of fluid flow for a laminar boundary layer (reference 7). This decrease in heat-transfer coefficient is caused by the formation of a cool boundary layer that serves to insulate the surface from the gas stream and thus decreases the amount of heat transfer.

This decrease in heat transfer can be defined by a decrease in effective gas temperature rather than a decrease in heat-transfer coefficient; but it is believed that defining the effective gas temperature using a recovery factor is a better procedure. The temperature gradient should then cause a decrease in heat-transfer coefficients along the trailing-edge section.

By using the analytical method incorporating a known effective gas temperature, this effect of decreasing heat-transfer coefficients can be experimentally determined by placing the thermocouple stations close together. By using the method where the effective gas temperature and the heat-transfer coefficients are simultaneously determined, the effective gas temperature would probably be abnormally low because of the effect of the cooled boundary layer, and the heat-transfer coefficient would be higher than for the case using a known effective gas temperature. The calculated rate of heat transfer to the blade would be the same in either case, but care should be exercised in evaluating the results obtained by the two different methods.

Accuracy Required in Locating Thermocouples

The distance between any two thermocouples used for measuring a temperature gradient should be known as accurately as possible because the errors ir the resulting data are in direct proportion to the error in the measurement of the distance between the locations where the temperature measurements are taken. Because thermocouples are usually located inside drilled holes, it is advantageous to have relatively shallow holes in order to reduce the amount of drift in the drilling operation as much as possible.

The location of the thermocouple junction in the hole is also of prime importance. The thermocouple junction should therefore be as small as possible and the junction itself should be in a hole of reduced diameter to insure the proper location of the junction. For

differential thermocouple readings, the junction must also be electrically insulated from the blade unless the blade is used as one of the elements of the thermocouple. The insulation should be thin to reduce the thermocouple time lag and it should be of such a nature that the location of the junction is also known. In general, errors resulting from improper thermocouple location and installation can be reduced by placing the thermocouples as far apart as possible consistent with other requirements of the installation and by placing the thermocouples in small shallow holes.

Effect of Thermocouple Hole on Heat-Flow Path

An analysis has not been made to evaluate the effects of holes placed in the heat path similar to those holes in which thermocouples are placed. If the holes are small compared to the wall thickness and if the metal beyond the thermocouple junction is solid, the errors caused by the holes are believed to be negligible.

Accuracy of Temperature Measurement

Accurate measurements of the temperature difference between two known locations in the blade metal are necessary. In most cases the difference between the two observed absolute temperature readings is not accurate enough. The method of measurement that has been found to be most successful is the use of a differential thermocouple circuit and the measurement of the potential from the circuit with a sensitive potentiometer and a light-beam galvanometer. Frequently, use of the blade metal as one of the thermocouple elements is convenient because differential readings can be made with the thermocouple wire bonded to the blade metal. The single-wire thermocouples can also be placed in smaller holes. In order to use this method of temperature-difference measurement, an accurate calibration of temperature against electromotive force must be made of the metals used to form the thermocouple.

The necessity for the high degree of accuracy required in the differential temperature measurements between two locations in the blade metal can be illustrated by equation (1a):

$$\Gamma = \frac{t_x - t_y}{t_e - t_x} \qquad (1a)$$

The outside heat-transfer coefficient is almost a linear function of Γ for the range encountered in most investigations so that the coefficient is directly proportional to $t_x - t_y$ and inversely proportional to $t_e - t_x$. The temperature difference $t_x - t_y$ can range from less than 1° to over 30° F depending on the blade-metal thermal conductivity and the distance between the locations where the measurements are made. A 1° error in reading this temperature difference can therefore amount to an error of from 3 to 100 percent in the heat-transfer coefficient. The temperature difference $t_e - t_x$ may range from 100° to 1000° F or higher, however, so that considerably larger errors can be tolerated in its measurement.

EXPERIMENTAL RESULTS

Preliminary heat-transfer runs were made to determine how successful these methods of analyzing heat-transfer data are in actual practice. For the sake of simplicity, a single symmetrical water-cooled blade having a chord and span of 6 inches was mounted in a test section with contoured walls as shown in figure 4. With this wall arrangement, the pressure distribution found on a typical reaction turbine blade can be simulated. A series of heat-transfer runs were made with heated air at temperatures ranging from 200° to 1000° F.

The leading edge, the trailing edge, and the central sections of the test blade were of shapes that could be used with the temperature-distribution equations presented herein. Multiple thermocouples were placed in the line of heat flow at the leading and trailing edges and single thermocouples were placed in the wall at the central portion of the blade. The circles on the blade sketch indicate the locations of the temperature measurements. The blade used for these heat-transfer determinations was made of aluminum, which has a relatively high thermal conductivity; because of its high thermal conductivity, the data obtained from the single thermocouples in the blade walls could not be used to evaluate local heat-transfer coefficients at the central portion of the blade. Experimental data are therefore given for only the leading and trailing edges.

Trailing-Edge Section

Heat-transfer data obtained from the temperature measurements in the trailing edge are shown in figure 5. The scatter in the

experimental data points is quite small and the data fall in small clusters. Each cluster represents a different gas temperature. In this case, data were taken at 200°, 400°, 600°, 800°, and 1000° F. Variable coolant-flow points are shown at each gas temperature. The equation of the experimental line was determined by the method of least squares and the intercept Ω on the abscissa was 0.954. With this value of Ω, the local effective gas temperature can be calculated at any of the observed gas temperatures in the series of runs represented on this plot.

The slope of the line representing the data is $-\Gamma$, which in this case is equal to -0.0477. A straight-line approximation of equation (25) for the trailing edge of this blade is

$$h_t \approx 0.3775\,\Gamma \qquad (25a)$$

From this approximate relation, the resulting local value of the outside heat-transfer coefficient at the trailing-edge section is 0.01802 (Btu/(°F)(sq ft)(sec)). The average outside coefficient for the entire blade was slightly higher than this value, which serves as a rough check on the magnitude of the trailing-edge coefficient.

If the effective gas temperature is calculated from the local blade recovery factor and the local Mach number, the calculated heat-transfer coefficients are lower than for the case where the effective gas temperature is calculated from the intercept on figure 5. The calculation for the quantity of heat transferred is the same in either case, however, as long as corresponding values of heat-transfer coefficient and effective gas temperature are used in the calculation. Because it is usually easier to calculate the effective gas temperature from a blade recovery factor, outside heat-transfer coefficients were also calculated at each gas temperature using this value of effective gas temperature.

The recovery factor for this blade at the trailing edge was 0.90 at a Mach number of 1.0. The Mach number was maintained constant at 1.0 for this series of runs. Use of these values in equation (52a) results in

$$t_e = 0.983\,T \qquad (52b)$$

A plot of outside heat-transfer coefficient against gas temperature where the effective gas temperature is defined by equation (52b) is shown in figure 6. The data points shown were obtained

from arithmetically averaged blade temperatures at each gas temperature. All the experimental data used in figure 5 were also used to obtain figure 6. The outside heat-transfer coefficient increases as the gas temperature increases and is from 2.5 to 16 percent less than the constant coefficient obtained from the plot on figure 5.

Leading-Edge Section

Heat-transfer data obtained from the temperature measurements in the leading-edge section of the blade are shown in figure 7 for gas temperatures from 200° to 800° F. The scatter in the data for the leading-edge section of the blade is considerably greater than that for the trailing-edge section (fig. 5). There are two explanations for this scatter: (1) The change in local heat-transfer coefficient with distance from the stagnation point is very rapid. In this blade, the heat-transfer coefficient was not measured directly at the stagnation point and any stream fluctuations that might cause the stagnation point to shift would materially affect the value of the local outside heat-transfer coefficient. (2) In addition to this condition, the coolant flow near the leading edge of the blade was unstable and caused the blade temperatures to be unstable also. In a previous discussion, small errors or fluctuations in the blade-temperature measurements were shown to affect the accuracy of the data; the effect is illustrated here.

At the leading edge of the blade, the value of Ω was found to be 0.940. The straight-line approximation of equation (20) for the leading-edge section of this blade is

$$h_t \approx 1.738\ \Gamma \qquad (20a)$$

By using this relation, the local heat-transfer coefficient at the leading-edge section was found to be 0.0441 (Btu/(°F)(sq ft)(sec)).

Theory for the leading edge of cylinders indicates that the heat-transfer coefficient at the leading edge should increase with increase in gas temperature for a constant weight rate of gas flow. The plot of heat-transfer data in figure 7 indicates that this trend is also present here because the data points could be best represented by a curved line. The data obtained at a gas temperature of 1000° F were not included in figure 7 because of this trend. The data points at gas temperatures from 200° to 800° F can be approximately represented by a straight line and were presented in this figure for illustrative purposes only.

For a more accurate determination of the heat-transfer coefficients, the leading-edge-section data were also calculated using effective gas temperatures calculated from the recovery factor and the Mach number. The Mach number at the leading edge was 0.37 and the local recovery factor was 0.87, so that from equation (52a)

$$t_e = 0.997\ T \qquad (52c)$$

A plot of heat-transfer coefficient against gas temperature at the leading edge of the blade where the effective gas temperature is defined by equation (52c) is shown in figure 8; for reference the heat-transfer coefficient obtained from figure 7 is shown as a dashed line.

The heat-transfer coefficient at the leading edge is dependent to a very large degree on the leading-edge configuration. The coefficient is lowest for a circular section, increases materially as the section becomes elliptical, and becomes infinite for the leading edge of a flat plate. The heat-transfer coefficients represented by the solid line on figure 8 lie between those calculated from theory for a circular section and an elliptical section with a major- to minor-axis ratio of 2. Although this fact cannot be used as an accurate check on the heat-transfer data at the leading edge, it shows that the data are in the right range and the trend of variation in gas temperature is verified.

CONCLUDING REMARKS

The analytical methods for the determination of local heat-transfer coefficients and effective gas temperatures present a convenient method for obtaining these data and the actual application of the equations to experimental data is relatively simple. The application of the equations for the various sections of the blade is made in a similar manner for each section, greatly increasing their utility.

Measuring the temperature gradient in the metal with two or more thermocouples whenever possible is advantageous because the analysis methods using one thermocouple are considered less accurate and considerably more difficult.

A desirable feature of these analytical methods is that they are not limited to turbine blades alone but can be used to determine local heat-transfer coefficients and effective temperatures for many other types of apparatus where the heat is being transferred through metal in a shape that can be approximated by the shapes discussed herein.

Lewis Flight Propulsion Laboratory,
National Advisory Committee for Aeronautics,
Cleveland, Ohio.

APPENDIX A

SYMBOLS

The following symbols are used in this report:

A		blade surface area, sq ft
B	$=$	$\sqrt{\frac{h_t}{k_B \sin \alpha}}$
C		constant
c_p		specific heat at constant pressure, Btu/(lb)(°F)
d		differential
E		quantity in equation for trailing-edge analysis (equation (30))
F		radiation geometry factor
$\mathscr{F}$		radiation geometry factor for gray surfaces
f		function
G		quantity in equation for trailing-edge analysis (equation (46))
H_0		Hankel function of zero order
H_1		Hankel function of first order
h		heat-transfer coefficient, Btu/(°F)(sq ft)(sec)
I		quantity in equation for trailing-edge analysis (equation (29))
i	$=$	$\sqrt{-1}$
J_0		Bessel function of zero order
J_1		Bessel function of first order

K,K'	constants of integration (function of h_t/k_B)
k	thermal conductivity, Btu/(^oF)(ft)(sec)
L	length, ft
M	Mach number
N	quantity in equation for trailing-edge analysis (equation (28))
n	exponent
P	total pressure, lb/sq ft absolute
p	static pressure, lb/sq ft absolute
Q	heat-flow rate, Btu/sec
q	heat-flow rate per unit length, Btu/(ft)(sec)
r	radius, ft
S	quantity in equation for trailing-edge analysis (equation (46))
T	total temperature, ^oR
t	temperature, ^oR
w	weight-flow rate, lb/sec
X'	constant of integration (function of h_t/k_B)
Y'	constant of integration (function of h_t/k_B)
y	distance from trailing edge, ft (figs. 1(d) to (f))
Z,Z'	constants of integration (functions of h_t/k_B)
α	trailing-edge wedge angle, deg
Γ	function of h_t/k_B, thermocouple location, and blade configuration

Γ' intercept on plot of $(1 - \Gamma)/w_c^n$ against Γ (fig. 3(b))

γ ratio of specific heats

δ thermocouple location dimension, ft (fig. 1(a))

$\overline{\delta}$ blade-wall thickness, ft (fig. 1(a))

ϵ emissivity

ζ f_1 (h_t/k_B, k_B, and blade dimensions)

η f_2 (h_t/k_B, k_B, and blade dimensions)

θ angle, radians

Λ recovery coefficient

$$\xi = 2B\sqrt{\left(y + \frac{\pi}{4}\tau\right) + \tau\left(\frac{1 - \tan\alpha}{2\tan\alpha}\right)}$$

$$\xi_b = 2B_b\sqrt{y + \tau\left(\frac{1 - \tan\alpha_b}{2\tan\alpha_b}\right)}$$

τ thickness, ft (figs. 1(d) to (f))

$$\varphi = \sqrt{\frac{2h_t}{k_B\tau}}$$

$$\Omega = \frac{t_e}{t_g}$$

Subscripts:

av average

B blade

b trapezoidal portion of trailing-edge section composed of trapezoid and rectangle (fig. 1(e))

b'	first trapezoidal portion of trailing-edge section composed of two trapezoids (fig. 1(f))
c	coolant
d	rectangular portion of trailing-edge section composed of trapezoid and rectangle (fig. 1(e))
d'	second trapezoidal portion of trailing-edge section composed of two trapezoids (fig. 1(f))
e	effective; subscript used with symbol for temperature to denote temperature effecting heat transfer
g	gas
i	inside blade surface
o	outside blade surface
r	radiation
T	thermocouple
t	combination of radiation and convection
w	radiating surface
x	local value at some location
y	local value at some location different from location of x
1,2, . . . 7	refer to thermocouple locations unless otherwise noted

APPENDIX B

DERIVATION OF HEAT-TRANSFER EQUATIONS

Central Section of Blade

The heat flow through the blade wall is assumed normal to the blade surface and the surface curvature small enough that the wall can be treated as a flat plate. By reference to figure 1(b) for symbols and dimensions, the following heat balance can be written:

$$\frac{Q}{A} = h_t(t_e - t_o) = \frac{k_B}{\bar{\delta}}(t_o - t_i) = \frac{k_B}{\delta}(t_B - t_i) = h_i(t_i - t_c) \tag{B1}$$

where

t_o metal temperature on outside surface of blade

t_i metal temperature on inside surface of blade

t_B metal temperature at distance δ from coolant passage

The following equations can be obtained from equation (B1):

$$t_o = \frac{k_B t_i + \bar{\delta} h_t t_e}{k_B + \bar{\delta} h_t} \tag{B2}$$

$$t_i = \frac{k_B t_o + \bar{\delta} h_i t_c}{k_B + \bar{\delta} h_i} \tag{B3}$$

$$\frac{\delta}{\bar{\delta}} = \frac{t_B - t_i}{t_o - t_i} \tag{B4}$$

When t_o and t_i are eliminated from equations (B2) to (B4),

$$t_B - t_c = \frac{h_t(k_B + \delta h_i)}{k_B(h_t + h_i) + \bar{\delta} h_t h_i}(t_e - t_c) \tag{B5}$$

If Γ is defined here as

$$\Gamma = \frac{h_t(k_B + \delta h_i)}{k_B(h_t + h_i) + \bar{\delta} h_t h_i} \tag{12}$$

then

$$t_B - t_c = \Gamma(t_e - t_c) \tag{5}$$

The effective gas temperature t_e in equation (5) is defined as the temperature that the test blade would assume if there were no heat transfer to or from the blade (reference 3). A blade recovery factor Λ_B that is a function of the blade configuration and Mach number can be obtained, so that the effective gas temperature can be determined from the equation

$$t_e = T\left(\frac{1 + \Lambda_B \frac{\gamma - 1}{2} M_B^2}{1 + \frac{\gamma - 1}{2} M_B^2}\right) \tag{B6}$$

Similarly, the gas-temperature reading from a shielded thermocouple placed in the gas stream ahead of the blade will be

$$t_g = T\left(\frac{1 + \Lambda_T \frac{\gamma - 1}{2} M_T^2}{1 + \frac{\gamma - 1}{2} M_T^2}\right) \tag{B7}$$

where

t_g observed gas temperature reading from thermocouple, $^\circ R$

T total gas temperature, $^\circ R$

Λ_T recovery factor for thermocouple

M_T Mach number at thermocouple

If

$$t_e = \Omega t_g \tag{4a}$$

where Ω is a constant of proportionality, from equations (B6), (B7), and (4a),

$$\Omega = \left(\frac{1 + \Lambda_B \frac{\gamma - 1}{2} M_B^2}{1 + \Lambda_T \frac{\gamma - 1}{2} M_T^2}\right)\left(\frac{1 + \frac{\gamma - 1}{2} M_T^2}{1 + \frac{\gamma - 1}{2} M_B^2}\right) \tag{B8}$$

In order to determine the effect of variations in local Mach numbers and recovery factors of the blade and the thermocouple, values of Ω were calculated for Mach numbers from 0 to 1.0 by use of values of recovery factors from 0.65 to 1.0. The maximum variation in Ω with Mach number was about $2\frac{1}{2}$ percent.

Combination of equations (5) and (4a) and division by t_g yield

$$\frac{t_B - t_c}{t_g} = \Gamma\left(\Omega - \frac{t_c}{t_g}\right) \tag{6}$$

For the case when two temperature measurements can be made to obtain the temperature gradient in the blade wall, as shown on figure 1(a), temperatures t_1 and t_2 at corresponding distances δ_1 and δ_2 can be substituted into equation (B5), which results in two equations. Subtraction of the equation involving t_2 from the equation involving t_1 results in

$$\frac{t_1 - t_2}{t_e - t_c} = \frac{h_t h_i(\delta_1 - \delta_2)}{k_B(h_t + h_i) + \bar{\delta} h_t h_i} \tag{B9}$$

Equation (B6) can also be written

$$\frac{t_1 - t_c}{t_e - t_c} = \frac{h_t(k_B + \delta_1 h_i)}{k_B(h_t + h_i) + \bar{\delta} h_t h_i} \tag{B10}$$

Subtraction of both sides of equation (B10) from unity and combination with equation (B9) to eliminate h_i give

$$t_1 - t_2 = \frac{\frac{h_t}{k_B}(\delta_1 - \delta_2)}{1 + \frac{h_t}{k_B}(\bar{\delta} - \delta_1)}(t_e - t_1) \tag{B11}$$

If Γ is now defined as

$$\Gamma = \frac{\frac{h_t}{k_B}(\delta_1 - \delta_2)}{1 + \frac{h_t}{k_B}(\overline{\delta} - \delta_1)} \tag{9}$$

then equation (B11) becomes

$$t_1 - t_2 = \Gamma(t_e - t_1) \tag{7}$$

Equation (B5) can be written

$$h_i = \frac{1}{\zeta\left(\frac{t_e - t_c}{t_e - t_B}\right) - \eta} \tag{2}$$

where

$$\zeta = \frac{1}{k_B}\left(\frac{k_B}{h_t} + \overline{\delta} - \delta\right) \tag{16}$$

and

$$\eta = \frac{1}{k_B}\left(\frac{k_B}{h_t} + \overline{\delta}\right) \tag{17}$$

If t_B in equation (2) is replaced by t_2, equation (16) becomes

$$\zeta = \frac{1}{k_B}\left(\frac{k_B}{h_t} + \overline{\delta} - \delta_2\right) \tag{10}$$

Leading-Edge Section of Blade

Heat is assumed transmitted from the gas stream to the blade coolant at the leading edge of the blade along a sector with an included angle $d\theta$, as shown in the leading-edge cross-sectional view in figure 1(c). It is assumed that no heat is transmitted in

a direction normal to the sector path from the gas to the coolant; this assumption has been verified by relaxation calculations for well-rounded leading-edge sections. The following heat-balance equations can now be written:

$$dq = (t_e - t_o)(r_o\ d\theta)h_t \tag{B12}$$

$$dq = (t_i - t_c)(r_i\ d\theta)h_i \tag{B13}$$

$$dq = r\ d\theta\ k_B \frac{dt_B}{dr} \tag{B14}$$

where

dq heat transferred along sector having included angle $d\theta$ per unit length normal to sector, Btu/(ft)(sec)

r, r_i, r_o radii to concentric arcs of circles

t_B blade temperature at any point in sector, ^oR

t_i inside-blade-surface temperature, ^oR

t_o outside-blade-surface temperature, ^oR

From equation (B14),

$$t_B = \frac{dq}{k_B\ d\theta} \log_e Cr \tag{B15}$$

Then

$$t_o = \frac{dq}{k_B\ d\theta} \log_e Cr_o \tag{B16}$$

and

$$t_i = \frac{dq}{k_B\ d\theta} \log_e Cr_i \tag{B17}$$

Subtracting equation (B17) from (B16) yields

$$dq = \frac{k_B\ d\theta}{\log_e \frac{r_o}{r_i}} (t_o - t_i) \tag{B18}$$

It is obvious that

$$\frac{t_o - t_i}{t_e - t_c} = \frac{t_o - t_i}{(t_e - t_o) + (t_i - t_c) + (t_o - t_i)} \tag{B19}$$

Combination of equations (B12), (B13), (B18), and (B19) yields

$$t_o - t_i = \frac{t_e - t_c}{1 + \frac{k_B}{\log_e \frac{r_o}{r_i}} \left(\frac{1}{h_t r_o} + \frac{1}{h_i r_i} \right)} \tag{B20}$$

Subtraction of equation (B17) from (B15) and division by (B18) give

$$\frac{t_B - t_i}{t_o - t_i} = \frac{\log_e \frac{r}{r_i}}{\log_e \frac{r_o}{r_i}} \tag{B21}$$

When equations (B13) and (B18) are combined,

$$t_i - t_c = \frac{k_B}{r_i h_i \log_e \frac{r_o}{r_i}} (t_o - t_i) \tag{B22}$$

Combination of equations (B20) and (B22) results in

$$t_i - t_c = \frac{k_B}{r_i h_i \log_e \frac{r_o}{r_i}} \left[\frac{t_e - t_c}{1 + \frac{k_B}{\log_e \frac{r_o}{r_i}} \left(\frac{1}{h_t r_o} + \frac{1}{h_i r_i} \right)} \right] \tag{B23}$$

From a combination of equations (B20) and (B21), it is found that

$$t_B - t_i = \frac{\log_e \frac{r}{r_i}}{\log_e \frac{r_o}{r_i}} \left[\frac{t_e - t_c}{1 + \frac{k_B}{\log_e \frac{r_o}{r_i}} \left(\frac{1}{h_t r_o} + \frac{1}{h_i r_i} \right)} \right] \tag{B24}$$

It is obvious that

$$t_B - t_c = (t_B - t_i) + (t_i - t_c) \tag{B25}$$

By combination of equations (B23) to (B25),

$$\frac{t_B - t_c}{t_e - t_c} = \frac{\log_e \frac{r}{r_i} + \frac{k_B}{h_i r_i}}{\log_e \frac{r_o}{r_i} + \frac{k_B}{h_t r_o} + \frac{k_B}{h_i r_i}} \tag{B26}$$

If two temperatures t_3 and t_4 are measured in the sector at points 3 and 4 at radii r_3 and r_4, these values can be substituted into equation (B26), which results in two equations - one for each temperature. Subtracting the equation involving t_4 from the equation involving t_3 yields

$$\frac{t_3 - t_4}{t_e - t_c} = \frac{\frac{r_o h_t}{k_B} \log_e \frac{r_3}{r_4}}{1 + h_t\left(\frac{r_o}{k_B} \log_e \frac{r_o}{r_i} + \frac{r_o}{h_i r_i}\right)} \tag{B27}$$

Equation (B26) can also be written

$$\frac{t_3 - t_c}{t_e - t_c} = \frac{h_t\left(\frac{r_o}{k_B} \log_e \frac{r_3}{r_i} + \frac{r_o}{h_i r_i}\right)}{1 + h_t\left(\frac{r_o}{k_B} \log_e \frac{r_o}{r_i} + \frac{r_o}{h_i r_i}\right)} \tag{B28}$$

Subtraction of both sides of equation (B28) from unity and combination with equation (B27) give

$$t_3 - t_4 = \left(\frac{\frac{r_o h_t}{k_B} \log_e \frac{r_3}{r_4}}{1 + \frac{r_o h_t}{k_B} \log_e \frac{r_o}{r_3}}\right)(t_e - t_3) \tag{B29}$$

If Γ is defined as

$$\Gamma = \frac{\frac{r_o h_t}{k_B} \log_e \frac{r_3}{r_4}}{1 + \frac{r_o h_t}{k_B} \log_e \frac{r_o}{r_3}} \tag{20}$$

equation (B29) can be written

$$t_3 - t_4 = \Gamma(t_e - t_3) \tag{18}$$

Combination of equations (18) and (4a) and division by t_g yield

$$\frac{t_3 - t_4}{t_g} = \Gamma\left(\Omega - \frac{t_3}{t_g}\right) \tag{19}$$

In order to determine the value of the inside heat-transfer coefficient h_i, both sides of equation (B26) are subtracted from unity and the equation is rearranged to yield

$$h_i = \frac{1}{\frac{r_i}{k_B}\left(\log_e \frac{r_o}{r} + \frac{k_B}{h_t r_o}\right)\left(\frac{t_e - t_c}{t_e - t_B}\right) - \frac{r_i}{k_B}\left(\log_e \frac{r_o}{r_i} + \frac{k_B}{h_t r_o}\right)} \tag{B30}$$

If ζ and η are defined as

$$\zeta = \frac{r_i}{k_B}\left(\frac{k_B}{h_t r_o} + \log_e \frac{r_o}{r}\right) \tag{21}$$

and

$$\eta = \frac{r_i}{k_B}\left(\frac{k_B}{h_t r_o} + \log_e \frac{r_o}{r_i}\right) \tag{22}$$

equation (B30) can be written

$$h_i = \frac{1}{\zeta\left(\frac{t_e - t_c}{t_e - t_B}\right) - \eta} \tag{2}$$

Trailing-Edge Section of Blade

The trailing-edge cross section of most turbine blades can be approximated by a trapezoid, a rectangle, or a combination of trapezoids and rectangles. Heat-transfer equations are given for each case.

Trapezoidal trailing-edge section. - The temperature distribution in a trapezoidal trailing-edge section of a turbine blade is derived in reference 4 and is given herein by the expression

$$\frac{t_e - t_B}{t_e - t_c} = \frac{h_i N}{I + h_i E} \tag{B31}$$

where

$$N = \frac{\xi_2}{2B^2 k_B}\left[H_1(i\xi_1)\, J_0(i\xi) + iJ_1(i\xi_1)\, iH_0(i\xi)\right] \tag{28}$$

$$I = iJ_1(i\xi_1)\, H_1(i\xi_2) - H_1(i\xi_1)\, iJ_1(i\xi_2) \tag{29}$$

$$E = \frac{\xi_2}{2B^2 k_B}\left[H_1(i\xi_1)\, J_0(i\xi_2) + iJ_1(i\xi_1)\, iH_0(i\xi_2)\right] \tag{30}$$

$$\xi = 2B\sqrt{\left(y + \frac{\pi}{4}\tau_1\right) + \tau_1\left(\frac{1 - \tan\alpha}{2\tan\alpha}\right)}$$

$$B^2 = \frac{h_t}{k_B \sin\alpha}$$

$$\alpha = \tan^{-1}\frac{\tau_3 - \tau_1}{2L}$$

ξ_1 evaluated for $y + \frac{\pi}{4}\tau_1 = 0$

ξ_2 evaluated for $y = L$

y, τ_1, τ_3, L shown on trailing-edge section for trapezoidal shape (fig. 1(d))

$\frac{\pi}{4}\tau_1$ correction term in equation for ξ to account for rounded end of wedge and considered more accurate than $\tau_1/2$ as given in reference 4.

If two temperatures, t_5 and t_6, are measured in the trailing edge at distances y_5 and y_6, as shown on figure 1(d), these values can be substituted into equation (B31), which results in two equations, one for each temperature. Subtraction of the equation involving t_5 from the equation involving t_6 leaves

$$\frac{t_5 - t_6}{t_e - t_c} = \frac{\frac{N_6 - N_5}{I} h_i}{1 + \frac{E}{I} h_i} \tag{B32}$$

where N_5 and N_6 are evaluated at the positions where t_5 and t_6 are measured. Replacement of t_B by t_5 and N by N_5 in equation (B31) and combination with equation (B32) result in

$$t_5 - t_6 = \frac{N_6 - N_5}{N_5} (t_e - t_5) \tag{B33}$$

If Γ is defined as

$$\Gamma = \frac{N_6 - N_5}{N_5} \tag{25}$$

equation (B33) becomes

$$t_5 - t_6 = \Gamma(t_e - t_5) \tag{23}$$

Division of both sides of equation (23) by t_g and combination of the result with equation (4a) yield

$$\frac{t_5 - t_6}{t_g} = \Gamma\left(\Omega - \frac{t_5}{t_g}\right) \tag{24}$$

Solving equation (B31) for h_i yields

$$h_i = \frac{1}{\frac{N}{I}\left(\frac{t_e - t_c}{t_e - t_B}\right) - \frac{E}{I}} \tag{B34}$$

Letting

$$\zeta = \frac{N}{I} \tag{26}$$

and

$$\eta = \frac{E}{I} \tag{27}$$

results in a transformation of equation (B34) to

$$h_i = \frac{1}{\zeta\left(\frac{t_e - t_c}{t_e - t_B}\right) - \eta} \tag{2}$$

Rectangular trailing-edge section. - The temperature distribution in a rectangular trailing-edge section is given in reference 4. In the notation of this report, the expression becomes

$$\frac{t_e - t_B}{t_e - t_c} = \frac{\frac{h_i}{k_B}\cosh \varphi\left(y + \frac{\pi}{4}\tau_1\right)}{\varphi \sinh \varphi\left(L_2 + \frac{\pi}{4}\tau_1\right) + \frac{h_i}{k_B}\cosh \varphi\left(L_2 + \frac{\pi}{4}\tau_1\right)} \tag{B35}$$

where

L_2, y, τ_1 shown on rectangular portion of trailing-edge section sketch (fig. 1(e))

$\frac{\pi}{4}\tau_1$ correction for semicircular end of trailing-edge section

and

$$\varphi = \sqrt{\frac{2h_t}{k_B \tau_1}}$$

If two temperatures t_5 and t_7 are measured in the trailing edge at distances y_5 and y_7, as shown on figure 1(e), these values can be substituted into equation (B35), resulting in two equations - one for each temperature. Subtraction of the equation involving t_5 from the equation involving t_7 leaves

$$\frac{t_5 - t_7}{t_e - t_c} = \frac{h_i \left[\cosh \varphi\left(y_7 + \frac{\pi}{4}\tau_1\right) - \cosh \varphi\left(y_5 + \frac{\pi}{4}\tau_1\right) \right]}{\varphi k_B \sinh \varphi\left(L_2 + \frac{\pi}{4}\tau_1\right) + h_i \cosh \varphi\left(L_2 + \frac{\pi}{4}\tau_1\right)} \quad \text{(B36)}$$

Replacement of t_B by t_5 and y by y_5 in equation (B35) and combination with equation (B36) result in

$$t_5 - t_7 = \frac{\cosh \varphi\left(y_7 + \frac{\pi}{4}\tau_1\right) - \cosh \varphi\left(y_5 + \frac{\pi}{4}\tau_1\right)}{\cosh \varphi\left(y_5 + \frac{\pi}{4}\tau_1\right)} (t_e - t_5) \quad \text{(B37)}$$

By letting

$$\Gamma = \frac{\cosh \varphi\left(y_7 + \frac{\pi}{4}\tau_1\right) - \cosh \varphi\left(y_5 + \frac{\pi}{4}\tau_1\right)}{\cosh \varphi\left(y_5 + \frac{\pi}{4}\tau_1\right)} \quad (33)$$

equation (B37) becomes

$$t_5 - t_7 = \Gamma(t_e - t_5) \quad (31)$$

Division of equation (31) by t_g and combination of the result with equation (4a) yield

$$\frac{t_5 - t_7}{t_g} = \Gamma\left(\Omega - \frac{t_5}{t_g}\right) \quad (32)$$

Equation (B35) can be solved for h_i, which results in

$$h_i = \frac{1}{\frac{\cosh \varphi\left(y + \frac{\pi}{4}\tau_1\right)}{k_B \varphi \sinh \varphi\left(L_2 + \frac{\pi}{4}\tau_1\right)}\left(\frac{t_e - t_c}{t_e - t_B}\right) - \frac{\cosh \varphi\left(L_2 + \frac{\pi}{4}\tau_1\right)}{k_B \varphi \sinh \varphi\left(L_2 + \frac{\pi}{4}\tau_1\right)}} \tag{B38}$$

By letting

$$\zeta = \frac{\cosh \varphi\left(y + \frac{\pi}{4}\tau_1\right)}{k_B \varphi \sinh \varphi\left(L_2 + \frac{\pi}{4}\tau_1\right)} \tag{34}$$

and

$$\eta = \frac{\cosh \varphi\left(L_2 + \frac{\pi}{4}\tau_1\right)}{k_B \varphi \sinh \varphi\left(L_2 + \frac{\pi}{4}\tau_1\right)} \tag{35}$$

equation (B38) becomes

$$h_i = \frac{1}{\zeta\left(\frac{t_e - t_c}{t_e - t_B}\right) - \eta} \tag{2}$$

Combination trapezoidal and rectangular trailing edge. - By writing equation (B35) for t_B and t_7, equating the two expressions, and solving them, the temperature distribution in the rectangular portion of the trailing edge can be written as

$$t_e - t_B = (t_e - t_7)\frac{\cosh \varphi\left(y + \frac{\pi}{4}\tau_1\right)}{\cosh \varphi\left(L_2 + \frac{\pi}{4}\tau_1\right)} \tag{B39}$$

where

t_B temperature at any point in rectangular portion

t_7 temperature at point where $y = L_2 = y_7$

The temperature distribution for any trapezoidal shape is given in reference 8, and in the notation of this report becomes

$$t_e - t_B = KJ_0(i\xi) + ZiH_0(i\xi) \tag{B40}$$

The integration constants K and Z are functions of h_1. At the junction of the two portions of the trailing edge, the metal temperature and the heat flow must be continuous; therefore relations between the integration constants can be written.

At the junction, the blade temperature is t_7; therefore

$$t_e - t_7 = KJ_0(i\xi_{b,1}) + ZiH_0(i\xi_{b,1}) \tag{B41}$$

where

$\xi_{b,1}$ evaluated for $y = 0$

and

$$\xi_b = 2B_b\sqrt{y + \tau_1\left(\frac{1 - \tan\alpha_b}{2\tan\alpha_b}\right)}$$

$$\alpha_b = \tan^{-1}\frac{\tau_3 - \tau_1}{2L_1}$$

For the heat flow to be continuous, the following relation must exist:

$$k_B A_b \frac{dt_b}{dy} = k_B A_d \frac{dt_d}{dy} \tag{B42}$$

but $A_b = A_d$ at the junction where the subscripts b and d refer to the portion of the trailing-edge section in figure 1(e).

Differentiating equations (B39) and (B40) with respect to y and substituting the result in equation (B42) result in

$$(t_e - t_7)\,\varphi_d \tanh\varphi_d\left(L_2 + \frac{\pi}{4}\tau_1\right) = \frac{2B_b^2}{\xi_{b,1}}\left[-KiJ_1(i\xi_{b,1}) + ZH_1(i\xi_{b,1})\right] \tag{B43}$$

Temperatures t_5 and t_7 at corresponding distances y_5 and y_7 can be substituted into equation (B39), which results in two equations. Subtracting the equation involving t_5 from the equation involving t_7 results in

$$t_5 - t_7 = \frac{\cosh \varphi_d\left(y_7 + \frac{\pi}{4}\tau_1\right) - \cosh \varphi_d\left(y_5 + \frac{\pi}{4}\tau_1\right)}{\cosh \varphi_d\left(L_2 + \frac{\pi}{4}\tau_1\right)} (t_e - t_7) \tag{B44}$$

Equation (B39) can also be written

$$t_e - t_5 = (t_e - t_7) \frac{\cosh \varphi_d\left(y_5 + \frac{\pi}{4}\tau_1\right)}{\cosh \varphi_d\left(L_2 + \frac{\pi}{4}\tau_1\right)} \tag{B45}$$

The rigorous solution to equations (B44) and (B45) is rather complex. From equations (23) and (31) it can be seen that the final solutions for the various shapes take on the general form

$$t_x - t_y = \Gamma(t_e - t_x) \tag{1}$$

where Γ is a function of the blade dimensions, the end conditions, and the ratio h_t/k_B.

The simplest method of solving equations (B44) and (B45) to get them in the general form of equation (1) is to calculate the slope Γ_d of a plot of $t_5 - t_7$ against t_5. In order for the slope to be constant it cannot involve h_1. The slope of the line is

$$-\Gamma_d = \frac{\frac{d(t_5 - t_7)}{dh_1}}{\frac{d(t_5)}{dh_1}} \tag{B46}$$

From equation (B44),

$$\frac{d(t_5 - t_7)}{dh_1} = - \frac{\cosh \varphi_d\left(y_7 + \frac{\pi}{4}\tau_1\right) - \cosh \varphi_d\left(y_5 + \frac{\pi}{4}\tau_1\right)}{\cosh \varphi_d\left(L_2 + \frac{\pi}{4}\tau_1\right)} \frac{dt_7}{dh_1} \tag{B47}$$

1347

and from equation (B45),

$$\frac{dt_5}{dh_i} = \frac{\cosh \varphi_d\left(y_5 + \frac{\pi}{4}\tau_1\right)}{\cosh \varphi_d\left(L_2 + \frac{\pi}{4}\tau_1\right)} \frac{dt_7}{dh_i} \tag{B48}$$

Then from equations (B46) to (B48),

$$\Gamma_d = \frac{\cosh \varphi_d\left(y_7 + \frac{\pi}{4}\tau_1\right) - \cosh \varphi_d\left(y_5 + \frac{\pi}{4}\tau_1\right)}{\cosh \varphi_d\left(y_5 + \frac{\pi}{4}\tau_1\right)} \tag{33a}$$

For the trapezoidal portion of the trailing-edge section in figure 1(e), the temperatures t_7 and t_6 can be substituted into equation (B41), which results in two equations. Subtracting one equation from the other and differentiating yield

$$\frac{d(t_7 - t_6)}{dh_i} = \frac{dK}{dh_i}\left[J_0(i\xi_{b,6}) - J_0(i\xi_{b,7})\right] + \frac{dZ}{dh_i}\left[iH_0(i\xi_{b,6}) - iH_0(i\xi_{b,7})\right] \tag{B49}$$

and

$$\frac{dt_7}{dh_i} = -\frac{dK}{dh_i} J_0(i\xi_{b,7}) - \frac{dZ}{dh_i} iH_0(i\xi_{b,7}) \tag{B50}$$

where

$\xi_{b,6}$ evaluated for $y = y_6$

$\xi_{b,7}$ evaluated for $y = y_7$ ($y_7 = 0$ for this case)

Division of equation (B49) by equation (B50) to obtain the value of the slope $-\Gamma_b$ for the trapezoidal part of the trailing edge results in

$$\Gamma_b = \frac{J_0(i\xi_{b,6}) - J_0(i\xi_{b,7}) + \frac{dZ}{dK}\left[iH_0(i\xi_{b,6}) - iH_0(i\xi_{b,7})\right]}{J_0(i\xi_{b,7}) + \frac{dZ}{dK} iH_0(i\xi_{b,7})} \tag{38}$$

The value of dZ/dK in equation (38) can be found from equations (B41) and (B43) as follows:

When equations (B41) and (B43) are differentiated with respect to h_1,

$$\frac{dt_7}{dh_i} = -\frac{dK}{dh_i} J_0(i\xi_{b,1}) - \frac{dZ}{dh_i} iH_0(i\xi_{b,1}) \tag{B51}$$

and

$$\frac{dt_7}{dh_i} \varphi_d \tanh \varphi_d\left(L_2 + \frac{\pi}{4} \tau_1\right) = \frac{2B_b^2}{\xi_{b,1}} \left[\frac{dK}{dh_i} iJ_1(i\xi_{b,1}) - \frac{dZ}{dh_i} H_1(i\xi_{b,1})\right] \tag{B52}$$

where

$\xi_{b,1}$ evaluated for $y = 0$

Elimination of dt_7/dh_i yields

$$\frac{dZ}{dK} = \frac{2B_b^2 \, iJ_1(i\xi_{b,1}) + \xi_{b,1} \varphi_d \left[\tanh \varphi_d\left(L_2 + \frac{\pi}{4} \tau_1\right)\right] J_0(i\xi_{b,1})}{2B_b^2 \, H_1(i\xi_{b,1}) - \xi_{b,1} \varphi_d \left[\tanh \varphi_d\left(L_2 + \frac{\pi}{4} \tau_1\right)\right] iH_0(i\xi_{b,1})} \tag{39}$$

Combination of two trapezoidal sections in trailing edge. - The temperature distribution in the trapezoidal portion b' is given in different form in reference 8 as

$$t_e - t_B = K' J_0(i\xi_{b'}) + Z' iH_0(i\xi_{b'}) \tag{B53}$$

and in portion d' the distribution is

$$t_e - t_B = X' J_0(i\xi_{d'}) + Y' iH_0(i\xi_{d'}) \tag{B54}$$

where

K', Z', X', Y' integration constants

$$\xi_{b'} = 2B_{b'} \sqrt{y + \tau_2 \left(\frac{1 - \tan \alpha_{b'}}{2 \tan \alpha_{b'}}\right)}$$

$$\alpha_{b'} = \tan^{-1} \frac{\tau_3 - \tau_2}{2L_1}$$

$$B_{b'} = \sqrt{\frac{h_t}{k_B \sin \alpha_{b'}}}$$

$$\xi_{d'} = 2B_{d'} \sqrt{\left(y + \frac{\pi}{4} \tau_1\right) + \tau_1 \left(\frac{1 - \tan \alpha_{d'}}{2 \tan \alpha_{d'}}\right)}$$

$$\alpha_{d'} = \tan^{-1} \frac{\tau_2 - \tau_1}{2L_2}$$

and

$$B_{d'} = \sqrt{\frac{h_t}{k_B \sin \alpha_{d'}}} .$$

Here again the integration constants are functions of h_i and at the junction of the two trapezoidal sections the metal temperature and heat flow must be continuous. The following relations between the integration constants can be written:

For temperature continuity,

$$K'J_0(i\xi_{b',1}) + Z'iH_0(i\xi_{b',1}) = X'J_0(i\xi_{d',2}) + Y'iH_0(i\xi_{d',2}) \tag{B55}$$

and for heat-flow continuity,

$$k_B A_{b'} \frac{dt_{b'}}{dy} = k_B A_{d'} \frac{dt_{d'}}{dy} \tag{B42a}$$

Differentiating equations (B53) and (B54) with respect to y and substituting in equation (B42a) yield

$$\frac{B_{b'}{}^2}{\xi_{b',1}}\left[-K'iJ_1(i\xi_{b',1}) + Z'H_1(i\xi_{b',1})\right]$$

$$= \frac{B_{d'}{}^2}{\xi_{d',2}}\left[-X'iJ_1(i\xi_{d',2}) + Y'H_1(i\xi_{d',2})\right] \qquad (B56)$$

where

$A_{b'} = A_{d'}$

$\xi_{b',1}$ evaluated for $y = 0$

$\xi_{d',2}$ evaluated for $y = L_2$

The equation for portion d' is

$$t_5 - t_7 = \Gamma_{d'}(t_e - t_5) \qquad (40)$$

From equation (38), the equation for $\Gamma_{d'}$ can be written by inspection:

$$\Gamma_{d'} = \frac{J_0(i\xi_{d',7}) - J_0(i\xi_{d',5}) + \frac{dY'}{dX'}\left[iH_0(i\xi_{d',7}) - iH_0(i\xi_{d',5})\right]}{J_0(\xi_{d',5}) + \frac{dY'}{dX'}\,iH_0(i\xi_{d',5})} \qquad (B57)$$

where

$\xi_{d',7}$ evaluated for $y = y_7$

$\xi_{d',5}$ evaluated for $y = y_5$

Y',X' integration constants for portion d' that replace integration constants K and Z for portion b in equation (38)

The equation for dY'/dX' can also be written by inspection from equation (39). If the rectangular portion d were removed from portion b (fig. 1(e)), the quantity $\left(L_2 + \frac{\pi}{4}\tau_1\right)$ in equation (39) would be equal to zero and the equation would reduce to

$$\frac{dZ}{dK} = \frac{iJ_1(i\xi_{b,1})}{H_1(i\xi_{b,1})} \tag{39a}$$

Because nothing is attached on the rear of portion d' on figure 1(f), the equation for dY'/dX' is

$$\frac{dY'}{dX'} = \frac{iJ_1(i\xi_{d',1})}{H_1(i\xi_{d',1})} \tag{B58}$$

where

$\xi_{d',1}$ evaluated for $y + \frac{\pi}{4}\tau_1 = 0$

and

$$\xi_{d'} = 2B_{d'}\sqrt{\left(y + \frac{\pi}{4}\tau_1\right) + \tau_1\left(\frac{1 - \tan\alpha_{d'}}{2\tan\alpha_{d'}}\right)}$$

A correction for the rounded end is included in equation (B58) but not in equation (39a).

Substitution of equation (B58) into (B57) and notation of the definition of N given in equation (28) yield

$$\Gamma_{d'} = \frac{N_7 - N_5}{N_5} \tag{42}$$

When the same process as before is used to obtain an equation for portion b' in the form

$$t_7 - t_6 = \Gamma_{b'}(t_e - t_7) \tag{43}$$

it is found that

$$\Gamma_{b'} = \frac{J_0(i\xi_{b',6}) - J_0(i\xi_{b',7}) + \frac{dZ'}{dK'}\left[iH_0(i\xi_{b',6}) - iH_0(i\xi_{b',7})\right]}{J_0(i\xi_{b',7}) + \frac{dZ'}{dK'}\, iH_0(i\xi_{b',7})} \tag{45}$$

The value of dZ'/dK' can be obtained from equations (B55) and (B56) by differentiating and grouping to yield

$$\frac{dK'}{dh_i} J_0(i\xi_{b',1}) + \frac{dZ'}{dh_i} iH_0(i\xi_{b',1}) = \frac{dX'}{dh_i}\left[J_0(i\xi_{d',2}) + \frac{dY'}{dX'} iH_0(i\xi_{d',2})\right] \tag{B59}$$

and

$$- \frac{dK'}{dh_i} iJ_1(i\xi_{b',1}) + \frac{dZ'}{dh_i} H_1(i\xi_{b',1})$$

$$= \frac{dX'}{dh_i}\left[- iJ_1(i\xi_{d',2}) + \frac{dY'}{dX'} H_1(i\xi_{d',2})\right]\frac{B_{d'}{}^2\xi_{b',1}}{B_{b'}{}^2\xi_{d',1}} \tag{B60}$$

Elimination of dX'/dh_i from equations (B59) and (B60) and substitution of the value of dY'/dX' from equation (B58) yield

$$\frac{dZ'}{dK'} = \frac{GiJ_1(i\xi_{b',1}) + SJ_0(i\xi_{b',1})}{GH_1(i\xi_{b',1}) - SiH_0(i\xi_{b',1})} \tag{46}$$

where

$$G = J_0(i\xi_{d',2}) + \frac{iJ_1(i\xi_{d',1})\, iH_0(i\xi_{d',2})}{H_1(i\xi_{d',1})}$$

and

$$S = \frac{B_{d'}{}^2\xi_{b',1}}{B_{b'}{}^2\xi_{d',1}}\left[\frac{iJ_1(i\xi_{d',1})\, H_1(i\xi_{d',2})}{H_1(i\xi_{d',1})} - iJ_1(i\xi_{d',2})\right]$$

REFERENCES

1. McAdams, William H.: Heat Transmission. McGraw-Hill Book Co., Inc., 2d ed., 1942.

2. Hottel, H. C.: Radiant Heat Transmission. Mech. Eng., vol. 52, no. 7, July 1930, pp. 699-704.

3. Johnson, H. A., and Rubesin, M. W.: Aerodynamic Heating and Convective Heat Transfer - Summary of Literature Survey. Trans. ASME, vol. 71, no. 5, July 1949, pp. 447-456.

4. Brown, W. Byron, and Monroe, William R.: Cooling of Gas Turbines. IV - Calculated Temperature Distribution in the Trailing Part of a Turbine Blade Using Direct Liquid Cooling. NACA RM E7B11d, 1947.

5. Wolfenstein, Lincoln, Maxwell, Robert L., and McCarthy, John S.: Cooling of Gas Turbines. V - Effectiveness of Air Cooling of Hollow Blades. NACA RM E7B11e, 1947.

6. Livingood, John N. B., and Sams, Eldon W.: Cooling of Gas Turbines. VI - Computed Temperature Distribution through Cross Section of Water-Cooled Turbine Blade. NACA RM E7B11f, 1947.

7. Chapman, Dean R., and Rubesin, Morris W.: Temperature and Velocity Profiles in the Compressible Laminar Boundary Layer with Arbitrary Distribution of Surface Temperature. Jour. Aero. Sci., vol. 16, no. 9, Sept. 1949, pp. 547-565.

8. Harper, D. R., 3d, and Brown, W. B.: Mathematical Equations for Heat Conduction in the Fins of Air-Cooled Engines. NACA Rep. 158, 1922.

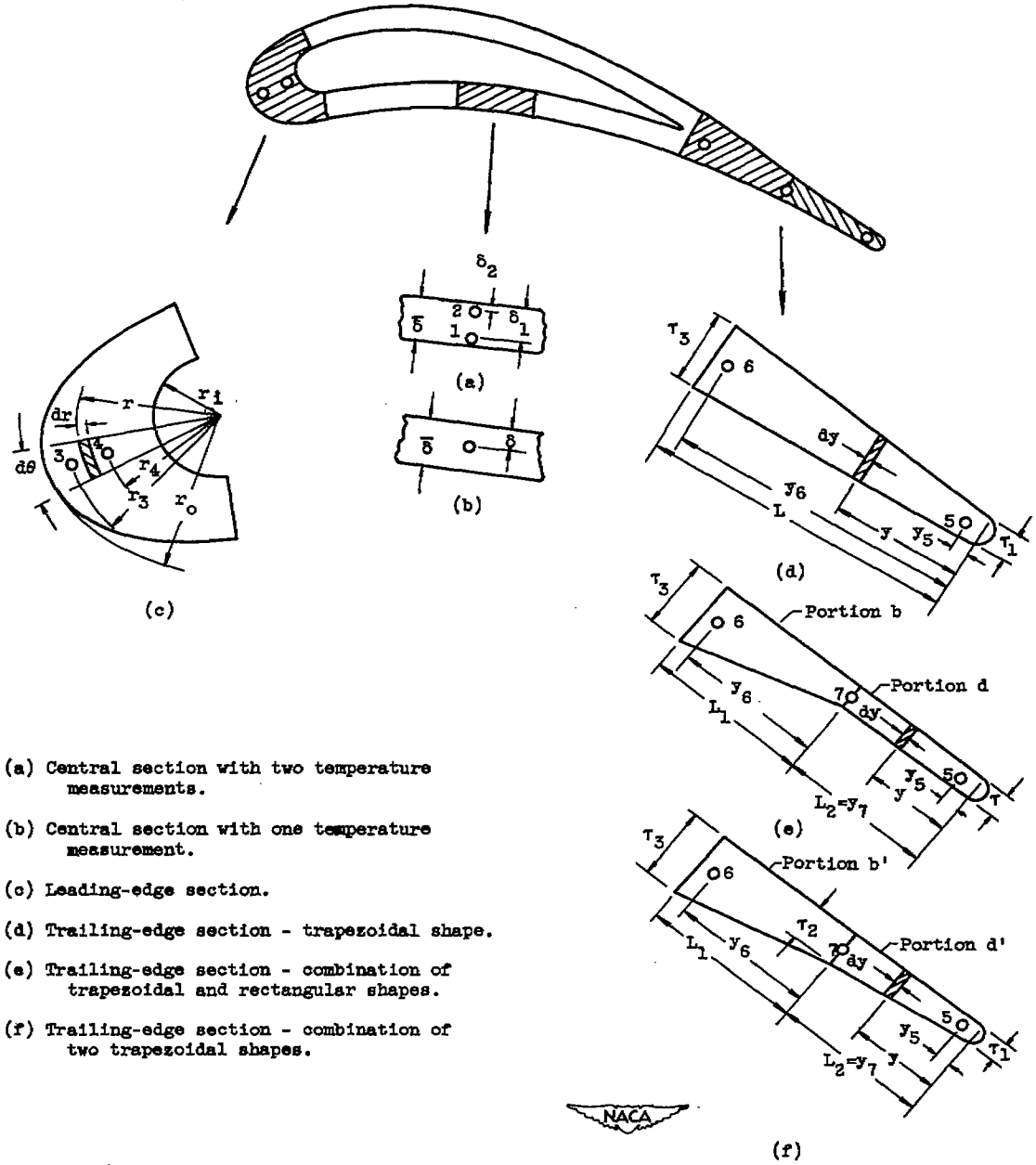

(a) Central section with two temperature measurements.

(b) Central section with one temperature measurement.

(c) Leading-edge section.

(d) Trailing-edge section - trapezoidal shape.

(e) Trailing-edge section - combination of trapezoidal and rectangular shapes.

(f) Trailing-edge section - combination of two trapezoidal shapes.

Figure 1. - Shape of turbine-blade sections for one-dimensional heat-transfer analysis.

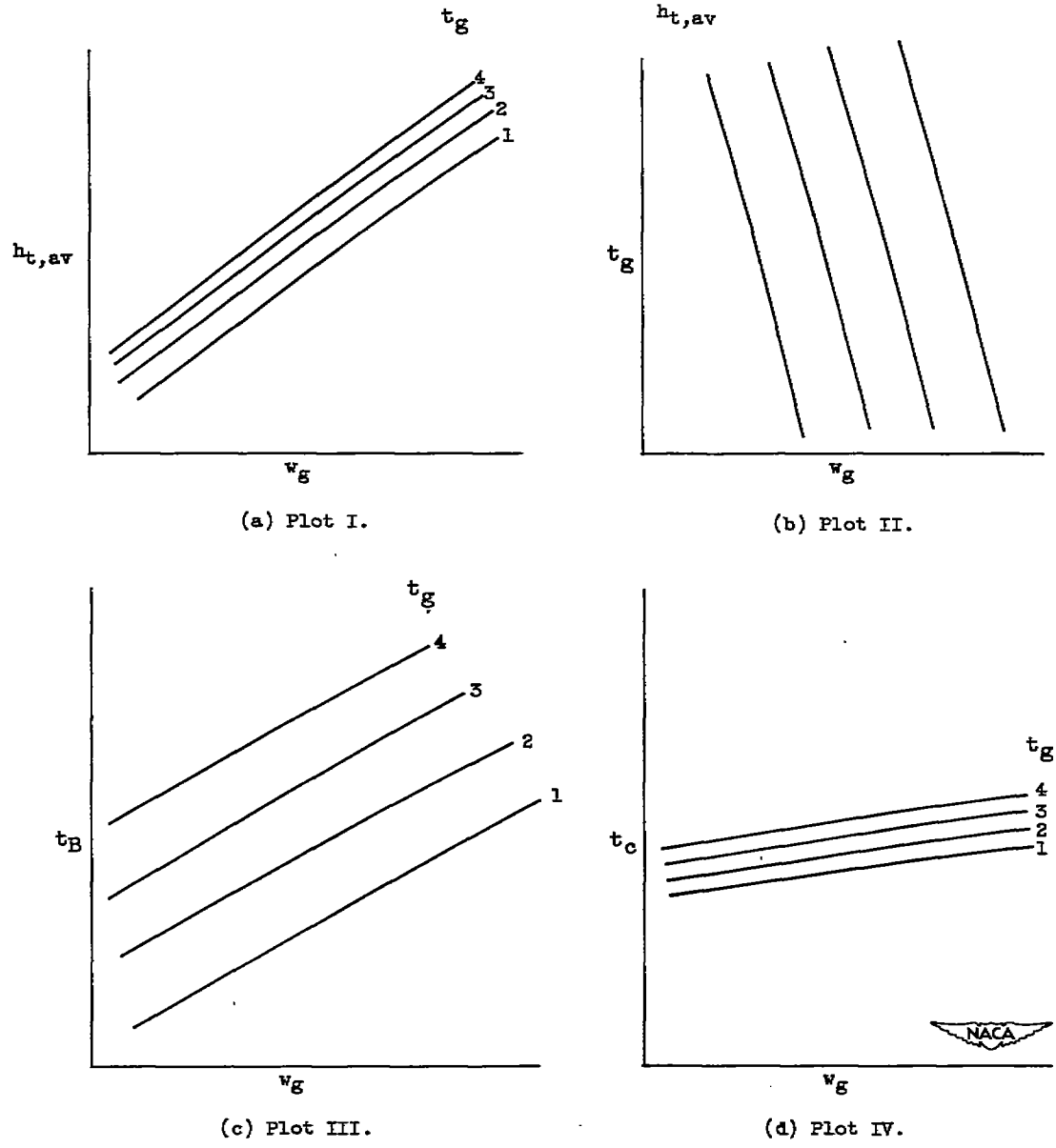

(a) Plot I.

(b) Plot II.

(c) Plot III.

(d) Plot IV.

Figure 2. - Illustrative plots to indicate method of determining turbine-blade and coolant temperatures for constant outside heat-transfer coefficient.

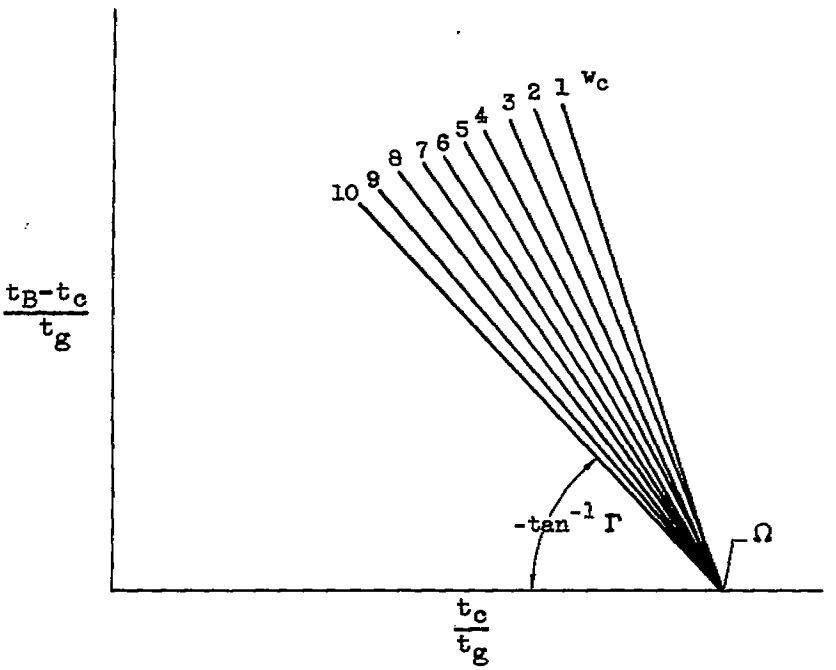

(a) Plot I.

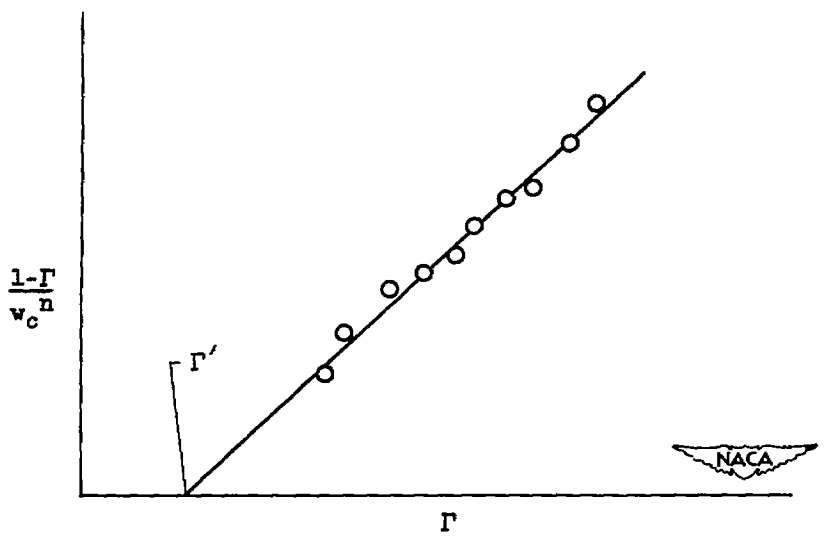

(b) Plot II.

Figure 3. - Illustrative graphical solution of temperature-distribution equation for central portion of blade using one thermocouple.

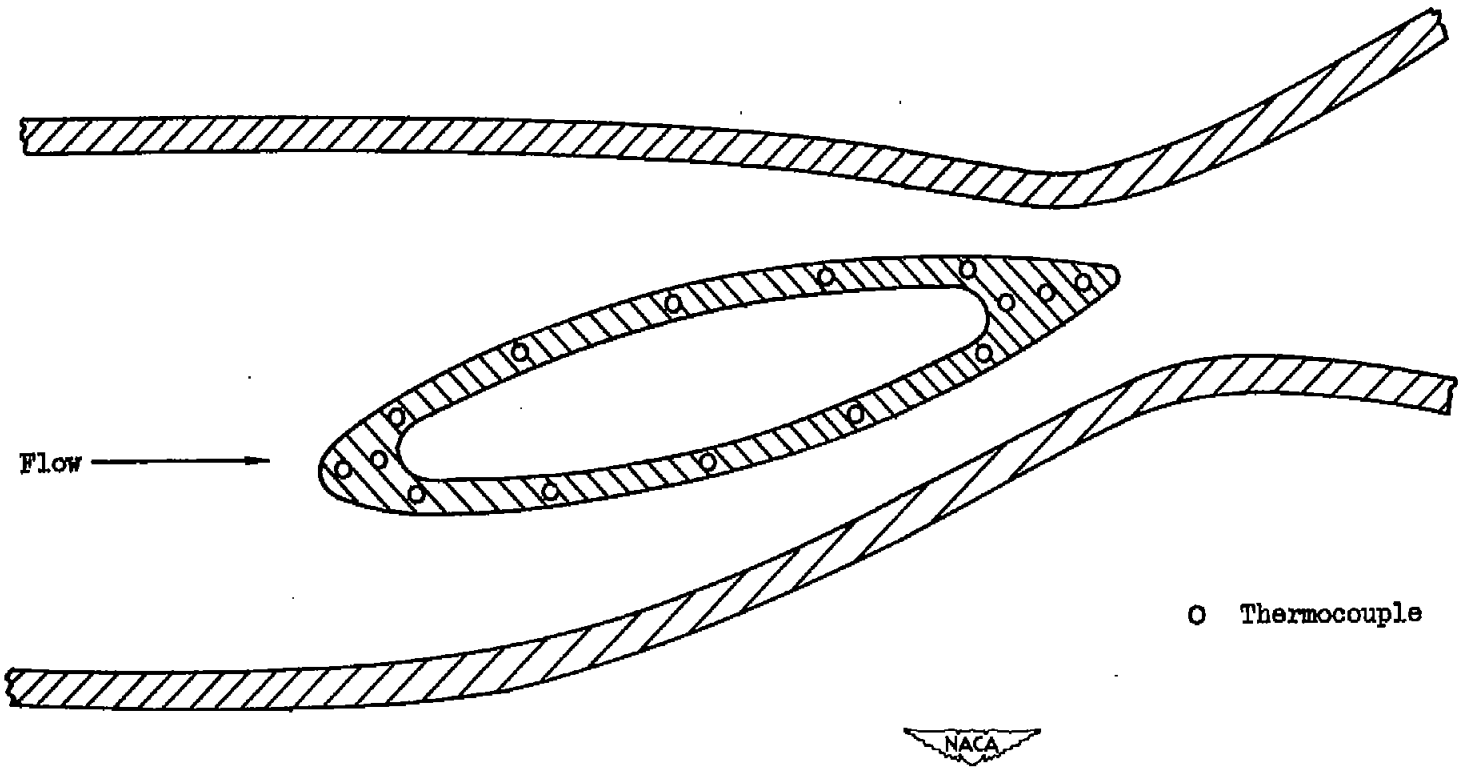

Figure 4. - Water-cooled blade used for experimental determination of local heat-transfer coefficients and effective gas temperatures.

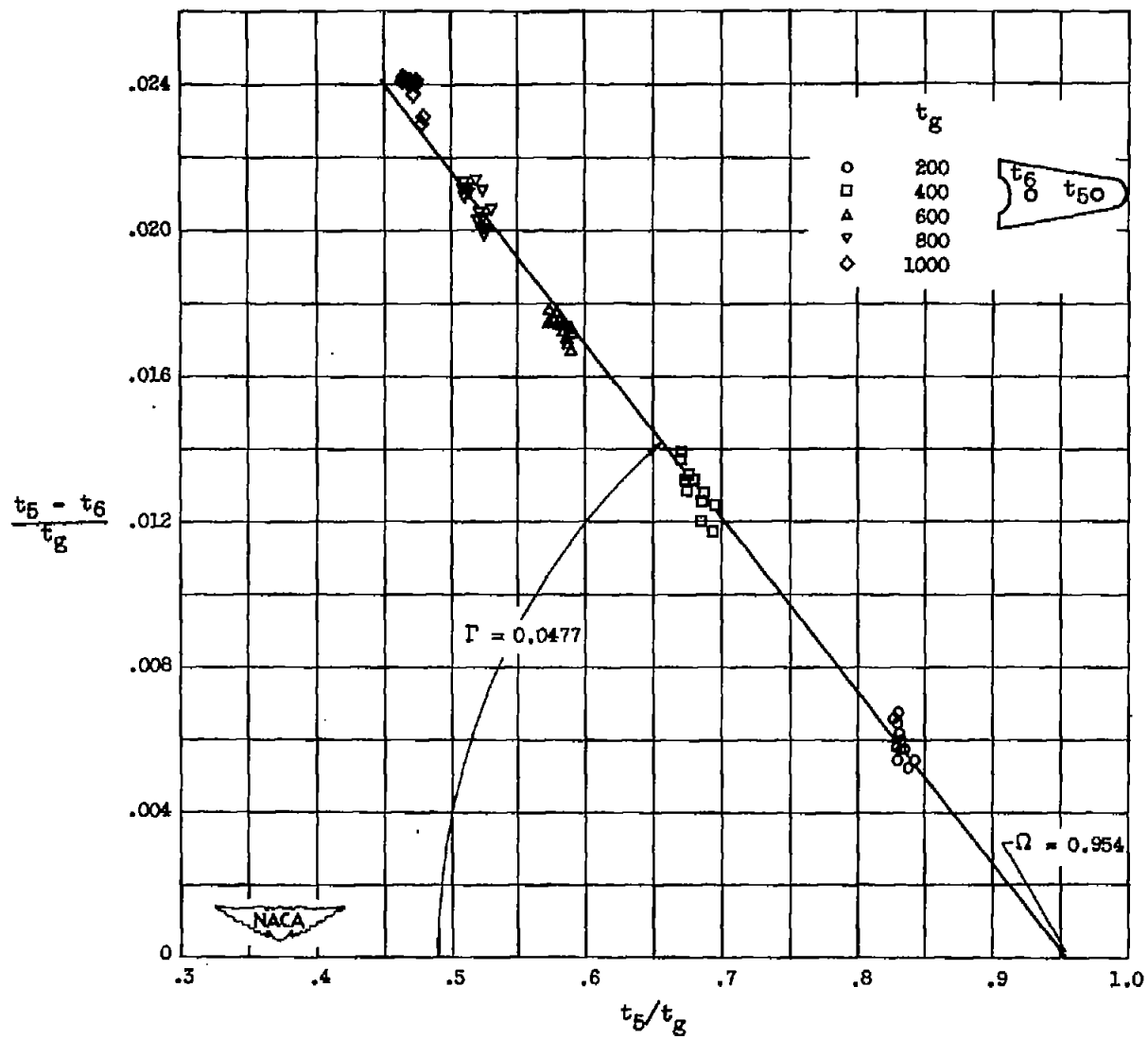

Figure 5. - Experimental determination of local outside-surface heat-transfer coefficient and effective gas temperature at trailing edge of water-cooled blade.

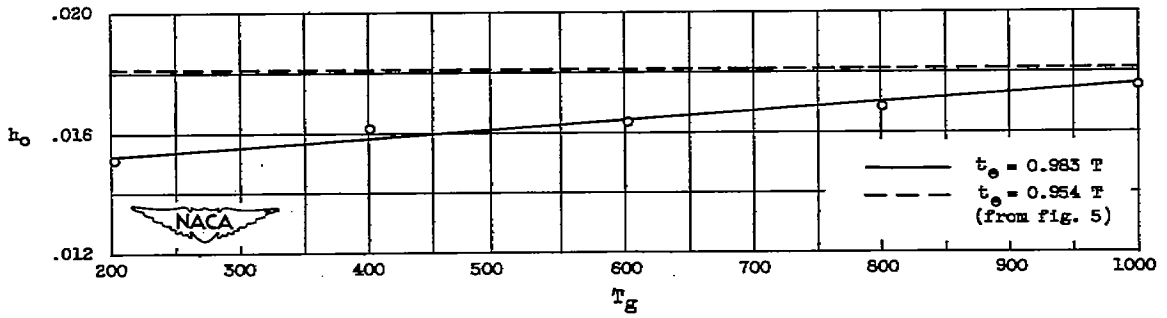

Figure 6. - Comparison of outside-surface heat-transfer coefficients at trailing edge of blade obtained from figure 5 with those calculated where the effective gas temperature was based on recovery factor.

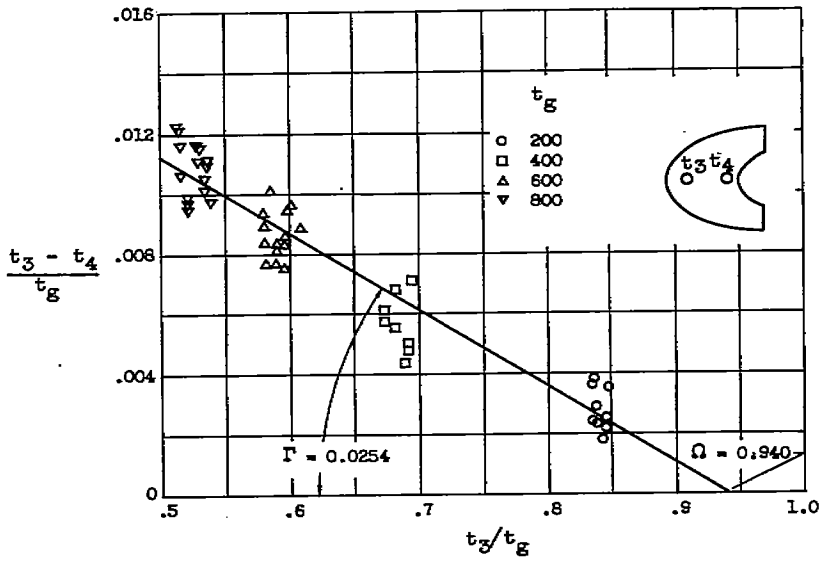

Figure 7. - Experimental determination of local outside-surface heat-transfer coefficient and effective gas temperature at leading edge of water-cooled blade.

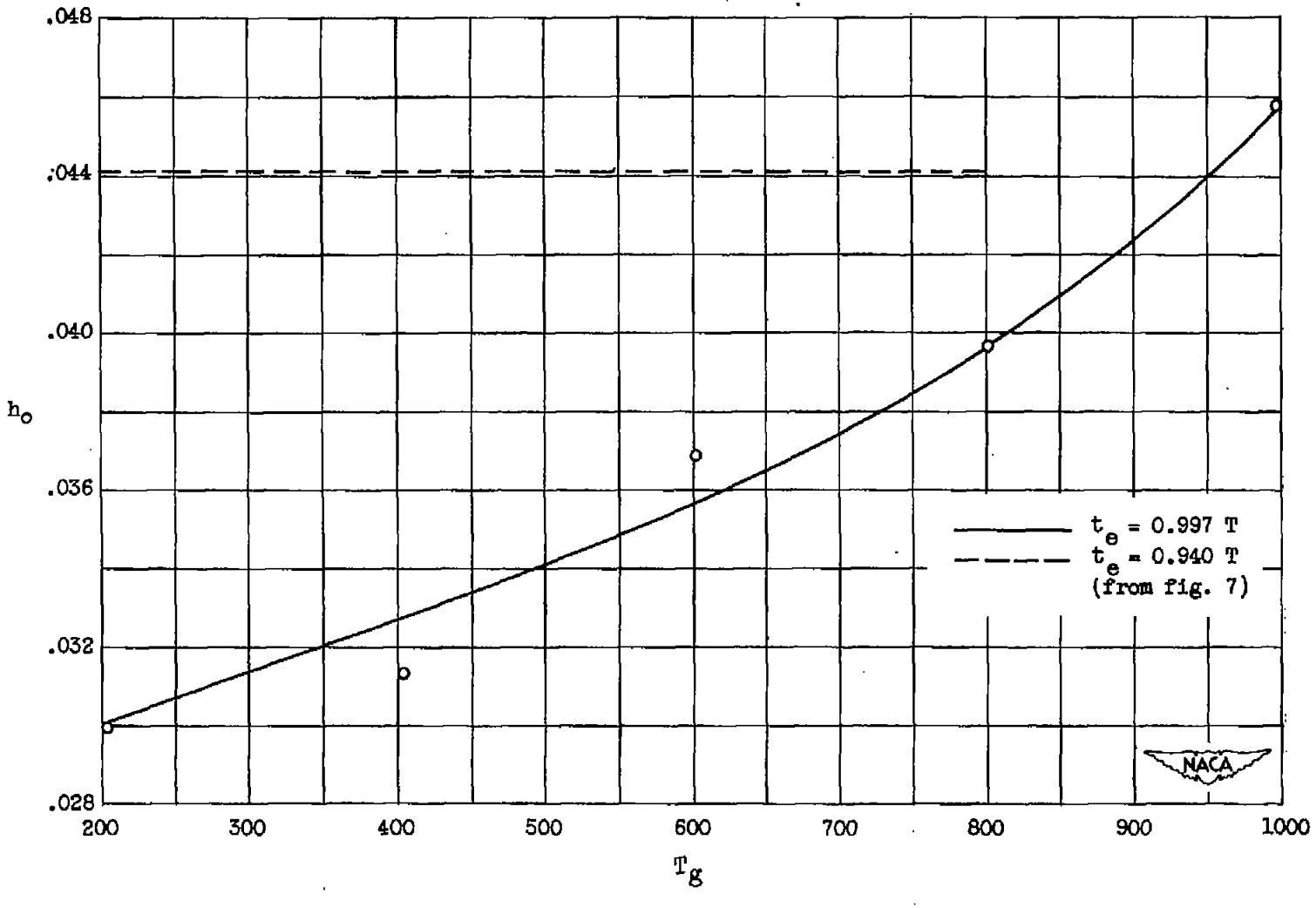

Figure 8. - Comparison of outside-surface heat-transfer coefficients at leading edge of blade obtained from figure 7 with those calculated where effective gas temperature was based on recovery factor.

NACA-Langley - 8-11-50 - 275